UNIVERSITY OF CALIFORNIA, SAN DIEGO

Induction of Vascular Smooth Muscle Lineage Differentiation by Shape Anisotropy: Role of microRNAs

A thesis submitted in partial satisfaction of the
requirements for the Degree of Master of Science

in

Bioengineering

by

Joshua Wei

Committee in charge:

Professor Shu Chien, Chair
Professor Adam Engler
Professor Peter Wang

2016

The thesis of Joshua Wei is approved, and is acceptable in quality and form for publication on microfilm and electronically:

_____

_____

_____

Chair

University of California, San Diego

2016

DEDICATION

For my parents, Joe and Catherine Wei, who continuously offer their love and support in everything I do.

TABLE OF CONTENTS

LIST OF FIGURES

ACKNOWLEDGEMENTS

My deepest gratitude goes to my advisor, Dr. Shu Chien for always making the time to offer his guidance and support throughout my time as a student. Also, this thesis would not have been possible without the help of Dr. Mark Wang, who offered advice and encouragement as both a mentor and a friend. The soft lithography fabrication and traction force experiments were much in thanks to Dr. Yi-Ting Yeh and del Álamo's Research Group in University of California, San Diego. I would also like to thank my thesis committee members, Dr. Adam Engler and Dr. Peter Wang, for their feedback and support.

The members of the entire Chien Lab also have my sincere thanks for their insightful questions and comments in lab meetings and various discussions. I would like to thank Dr. Julie Li for her offering new perspectives on problems and aiding me greatly during my writing process. I also want to thank Dr. Jason Haga and Phu Nguyen for mentoring me as my years as an undergraduate.

And finally, my greatest support throughout my life has always been my parents, Joe and Catherine Wei. They have always put my needs before their own and without them, I would not be the person who I am today.

ABSTRACT OF THE THESIS

Induction of Vascular Smooth Muscle Lineage Differentiation by Shape Anisotropy: Role of microRNAs

by

Joshua Wei

Masters of Science in Bioengineering

University of California: San Diego, 2016

Professor Shu Chien, Chair

Contractile vascular smooth muscle cells (VSMCs) sourced from donors are limited in supply for vascular tissue research and autologous transplantation therapies. Protocols using biochemical signaling for the derivation of functional, contractile SMCs from human induced pluripotent stem cells (hiPSCs) and mesenchymal stem cells (MSCs) have recently been explored, but they do not induce the full SMC phenotype. Biochemical cues are just one type of signaling that occurs *in vivo* and more thorough differentiation protocols could be developed through understanding the biomechanical effects of external forces resulting from shape modulation and surface topography. The goal of this study is to delineate the induction mechanism of biomechanical shape modulation and identify the key post-transcription regulators through the study of microRNAs and how they affect differentiation pathways in response to external stimuli. Of particular interest are miR-27 and miR-145, whose roles in MSC to VSMC differentiation are not yet fully established. To study the roles of miR-145 and miR-27 in regulating the shape

modulation-induced MSC-to-VSMC differentiation, MSCs were cultured onto 10-μm wide microgrooves fabricated through soft lithography over a 3-day period with TGF-β supplemented growth media. The synergistic SMC inductions of both biochemical and biomechanical signals were validated through the increases of SMC marker expression and contractile phenotype, which were quantified by Western blot, RT-qPCR, and cell traction force microscopy. Finally, the changes of myogenesis-related miRNAs were profiled by miRNA RT-qPCR, and gain-of-function and loss-of-function experiments on miR-27 and miR-145 were performed to evaluate their roles in the biomechanical induction of VSMC differentiation. These studies were conducted to elucidate roles of miR-27 and miR-145 in modulating SMC phenotype in response to biomechanical and biochemical cues and advance our ability to control stem cell (SC) induction into VSMCs. The findings have implications in a broad range of bioengineering applications, including vascular pathophysiology and graft tissue engineering .

CHAPTER 1. INTRODUCTION

1.1 Overview

There is an increasing need to study stem cell maintenance and differentiation for a better understanding of their cellular mechanisms and the potential applications in stem cell therapies. One of the gaps in our knowledge is the differentiation of VSMCs from MSCs, which are multipotent precursors of VSMCs. The differentiation process is still poorly defined, and further study would be crucial to therapies related to vascular regeneration, angiogenesis, and treatment of diseases such as neointimal hyperplasia. Differentiation requires a complex interaction of environmental cues, including biochemical stimuli, cell-cell interactions, cell-ECM interactions, and external mechanical factors. This work seeks to isolate and study specifically the effect of biomechanical factors resulting from shape anisotropy on MSCs and their signaling pathways. There are a variety of mechanical factors that help determine cell fate such as substrate stiffness and mechanical stresses. By isolating the effects of cell geometry and modulating this cue, new insights on how cell elongation impacts its phenotype may be gained. In this research, I hope to elucidate the mechanisms governing and regulating VSMC differentiation in response to changes in cell shape, especially its elongation and anisotropy.

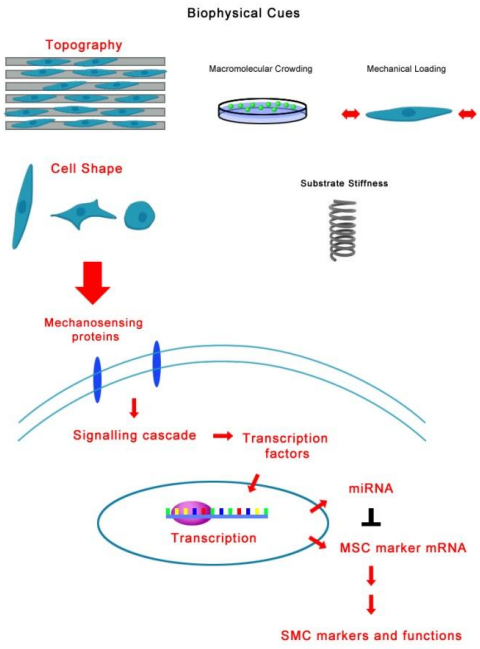

Fig. 1 - Regulators of MSC-to-VSMC differentiation
Many factors help regulate the differentiation process, but the involvement of mechanical stimuli has yet to be fully characterized. Of particular interest in this study are the effects of MSC geometry in VSMC differentiation due to modulation by substrate topography.

1.2 Angiogenesis and mesenchymal stem cells

In order to sustain its normal functions, the human body relies on an intricate system of blood vessels through which blood is continuously pumped by the heart. New vasculature is constantly generated in a developing embryo and in response to wound healing. Angiogenesis, the process of growth and development of new blood vessels from preexisting vessels, is mediated by factors such as VEGF (vascular endothelial growth factor), ANG2 (angiopoitin-2), TGF-α (transforming growth factor-α) and FGF (fibroblast growth factor). In response to appropriate stimuli, endothelial cells (ECs) migrate into the growth area, begin proliferation and tube formation, and signal for the recruitment of mural cells (pericytes and smooth muscle cells) as the vessel walls mature[1]. The development of smooth muscles (SMs) begins with

chemoattractants released by the ECs, signaling various SM progenitor cells such as mesenchymal stem cells (MSCs) to invest onto the vessel wall[1]. MSCs are multipotent stem cells that are present in various tissue types such as adipose tissues and bone marrow, as well as amniotic fluid. The MSCs commit and differentiate into SMCs as they make contact with the EC layer, losing their proliferative ability as progenitor cells[1]. MSCs have been defined by the international Society for Cell Therapy using several minimal criteria: The cells must adhere to plastic substrates in standard culture conditions; they must express surface molecules CD73, CD90, and CD105 while lacking CD34, CD45, CD14 or CD11b, CD79a or CD19, and HLA-DR; and they must be able to differentiate into osteoblasts, adipocytes, and chondroblasts under *in vitro* culture conditions[2]. Because MSCs are multipotent precursor cells to VSMCs, they are chosen as a model in the present study.

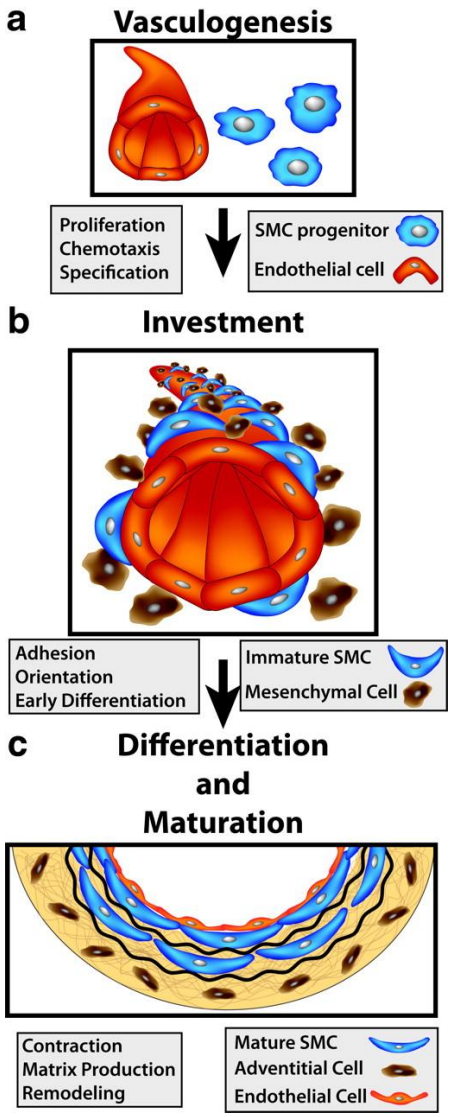

Fig. 2 - Angiogenesis and mural cell recruitment
Mural cells are recruited from precursor cells circulating in the blood stream, namely MSCs. They cover the arteries, veins, and capillaries to mature and stabilize the blood vessels. The new VSMCs require several steps of further maturation before they acquire their full contractile functionality and gene expression profile. (Adapted from M. Majesky et al.[3])

1.3 Vascular smooth muscle cells and smooth muscle differentiation

Cellular differentiation is the process in which potent cells develop characteristics that differentiate them from other cell types due to their specific phenotypes. This requires the activation of a certain set of cell-specific genes that are continuously regulated by environmental cues in order to differentiate and maintain the epigenetic programming of the

cell. This will influence not only the gene expression and cellular function, but also cell interaction with its environment, impacting the tissue and organ morphogenesis. Thus, it is important to first categorize the phenotype of VSMCs in order to discern them from other cell types. VSMCs display a broad range of phenotypes that correspond to their stages in development. However, adult cells do not necessarily exhibit a terminal phenotype, and have the ability to plastically modify their phenotype between the contractile and synthetic phases. In the synthetic phase, the VSMCs are more proliferative, become migratory, and lose their contractile function; they express genes that indicate a relatively dedifferentiated state. Adult SMCs in the contractile phase show little proliferation and display proper receptors, regulatory proteins, and contractile structures required for its functional needs[4]. SMCs can switch between these two phases in response to a multitude of environmental cues, including humoral factors, atherogenic/pathogenic stimuli, neuronal control, and their interaction with the extracellular matrix (ECM), ECs, and other SMCs, and mechanical forces[5]. The plastic nature of SMCs in response to outside cues is critical for proper injury response and subsequent vascular development and maturation. The conversion of contractile SMCs to synthetic SMCs greatly speeds the repair of damaged vessel and the replacement of missing SMCs. The synthetic SMCs release matrix-digesting enzymes, migrate to focal lesions, increase the rate of proliferation, and synthesize new ECM[6]. After the environment stabilizes, synthetic SMCs revert back to the contractile phase and resume contractile function.

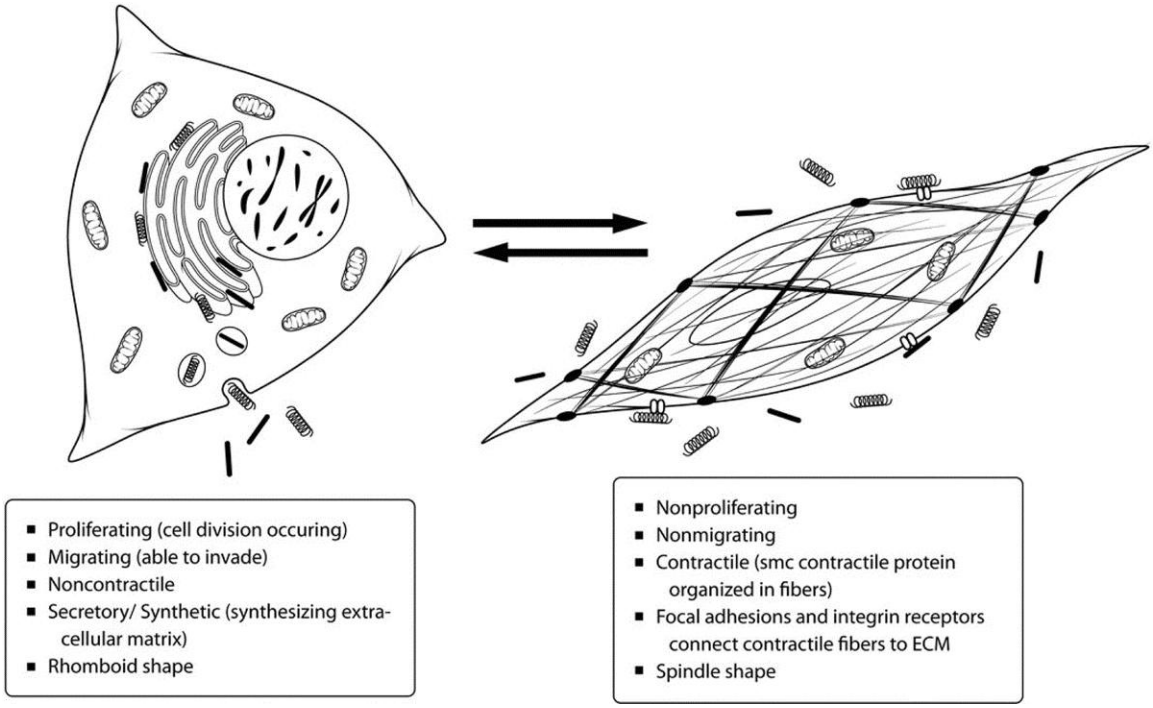

Fig. 3 - Phenotype plasticity of SMCs
SMCs can display a spectrum of phenotypes ranging between the contractile and synthetic phases. The right represents the fully differentiated and highly contractile phase whereas the left represents the highly synthetic phase. The ultimate phenotype of an SMC depends on a complex interaction of many types of local environmental cues ranging from biomechanical to humoral. Two arrows between the cells represent the two separate pathways involved in the phenotypic transition, the details of which remain unclear[5]. Their cell shape also vary greatly as synthetic SMCs are much rounder in shape while contractile SMCs have a spindle shape. (Adapted from D. Milewicz et al.[6])

In fully mature contractile SMCs, SMC phenotypic markers such as SM α-actin (SMA), SM-calponin (CNN1), SM22, and SM-myosin heavy chain (MYH11) can be observed in the cytoskeleton and contractile protein structures[3]. Genes linked to the SMC lineage have been found to be heavily mediated by the transcription factor SRF (serum response factor), a mcm-agamous-deficiens-srf (MADS) box–containing DNA binding protein[7]. SRF activates SM genes through a highly conserved 10-bp *cis*-element known as the CArG box[8]. Its MADS domain also allows for regulation by other signal molecules and proteins, especially the MYOCD (myocardin) family of proteins, which proves vital for VSMC differentiation and the formation of contractile protein structures[7]. MYOCD forms a stable ternary complex with SRF to coactivate transcription

of muscle-specific target genes[9]. MYOCD is expressed across SMCs of the cardiovascular system and internal organs as a critical coactivator, but is inactive without the required cofactor.

MSCs are known to have two main differentiation pathways, the Wnt canonical pathway and the TGF-β superfamily pathways. TGF-β has been shown to induce contractile phenotype through the regulation of SRF and its cofactor MLK1[10, 11]. It also facilitates cell differentiation by inducing changes in cell morphology and the actin filament structures, opening up pathways for cell remodeling[12]. These effects alone are not sufficient to induce a full VSMC phenotype. The compounded effect of many environmental factors is required, making VSMC differentiation difficult to achieve *in vitro*. Other studies have found that administering vascular endothelial growth factor (VEGF) and platelet-derived growth factor BB (PDGF-BB) to Flk1+ cardiovascular progenitor cells triggers the upregulation of SMA and the induction of spindle-like cell shape[13]. It has also been shown that EC interaction is crucial in initiating SM differentiation pathways through the induction of activin A expression[14]. Recent, differentiation protocols have used a combination of these interactions and growth factors to differentiate and maintain VSMCs with reasonable success[15]. However, there are still many interactions related to the differentiation pathway that are not yet understood.

1.4 Biomechanical factors and their roles in VSMC differentiation

Despite current understanding of MSCs and their propensity for VSMC differentiation, the differentiation process is still not reliably reproducible in laboratory settings, as current differentiation protocols cannot account for the full range of biomechanical forces that occur *in vivo*. MSCs are known to lose certain markers and gain others when cultured *in vitro*, suggesting a change in phenotype triggered by the altered environment[16]. This is because stem cell propensity is not only regulated by biochemical effects, but also by a dynamic array of

biomechanical signals. These signals include force loading, shear stress, substrate stiffness, macromolecular crowding, substrate topography, cell shape, etc. In order for these signals to translate into transcriptional changes in the nucleus, the cell utilizes a complex system of mechanosensing mechanisms involving integrin-mediated focal adhesions and actomyosin-based cytoskeleton structures[17]. To delineate the effects of certain biomechanical cues, studies must carefully design the microenvironment to include the signaling aspects of the extracellular matrix during cell fate determination. For example, Kurpinski et al. subjected MSCs to uniaxial strain while they were aligned by microgroove seeding to observe the anisotropic mechanosensing ability of the cell[18]. This led to increased CNN1 gene expression and MSC proliferation, while cartilage matrix markers were decreased[18]. Chromatin organization through dynamic tensile loading has been shown to establish 'mechanical memory' in MSCs, affecting how cells can react to future mechanical events and have long-term consequences for cell fate specification[19]. MSCs can be switched to a different lineage program through changing the stiffness of their hydrogel substrate, demonstrating plasticity in response to temporally changing cues[20]. These MSCs began to adopt morphologies that coincided with the functional features of their specific lineage fates[20]. This can be seen in SMC differentiation as contractile VSMCs restructure into a spindle-like shape to facilitate their function. Thus, extra attention was paid to cell morphology and its role in VSMC differentiation over the course of this study.

1.5 Pathology of smooth muscle

Understanding the regulation of VSMC differentiation and phenotypic plasticity has major implications in vascular repair and pathological development. The loss of VSMC function and increase in proliferation is notably connected to atherosclerosis and restenosis after angioplasty, both being severe and potentially fatal conditions. Atherosclerotic lesions develop as a response to intimal injury to cause ECs, platelets and inflammatory cells to release growth factors and cytokines that induce the synthetic phase of nearby VSMCs[21, 22]. The continuation of the lesion response promotes VSMC migration, proliferation, extracellular matrix (ECM) restructuring and deposition, and secretion of pro-inflammatory cytokines and growth factors[22, 23]. Plaque rupture related to the increased VSMC apoptosis can result in arterial thrombosis. Thus, the regulation of VSMC phenotype is a potential therapeutic target[24]. One approach highly relevant to this would be delineate and regulate the mechanisms through which geometrical stimuli mitigate the dedifferentiated VSMC pathological phenotype. Chang et al. successfully restored contractile phenotype of VSMCs *in vitro* by culturing cells on a micropatterned substrate[25]. My study aims to assess these same effects in MSCs and identify post-transcriptional regulators that modulate these processes, thus offering promising insights and avenues for future therapeutics for proliferative vasculopathy.

1.6 Post-transcriptional regulators: microRNA

While mechanotransduction steers cell fate through a variety of regulatory mechanisms, recent interest has brought to light the importance of microRNAs (miRNAs) in gene expression and regulation. miRNAs are post-transcriptional regulators that are responsible for the balance of many cellular events. Typically containing 20-25 nucleotides, these small non-coding RNA molecules play important roles in cell differentiation, proliferation and apoptosis by targeting

and regulating mRNAs through transcript degradation or translational repression[26]. miRNAs are first transcribed and processed in the nucleus as a single-stranded pre-miRNA hairpin before being exported into the cytoplasm (Fig. 4)[27]. Here, the terminal loop is spliced off by canonical Dicer enzyme in complex with TRBP (human immunodeficiency virus transactivating response RNA-binding protein) to form a miRNA/miRNA* duplex[28, 29]. The duplex is split and the more stable of the two single-stranded miRNAs is loaded into a miRNA RNA-inducing silencing complex (miRISC) by associating with Argonaute proteins (AGO)[27]. The miRISC silences gene expression binding to the 3' untranslated region of the target messenger RNA (mRNA), at a sequence-specific seed region. The miRNAs bind to mRNA following Watson-Crick base pairing (G-C and A-U), but bulges and mismatches generally occur[27]. The miRISC-mRNA complex prevents ribosomes from initiating translation of the mRNA and may induce deadenylation and subsequent degradation of the target[26]. Translational repression is considered the main mechanism in miRNA silencing, though complete complementary pairing of the miRNA is considered to lead to mRNA destabilization[27]. As a result, miRNAs are key negative regulators that play important role in tissue development and have potential as therapeutic targets, but their direct targets and full consequences of their actions are not all well characterized.

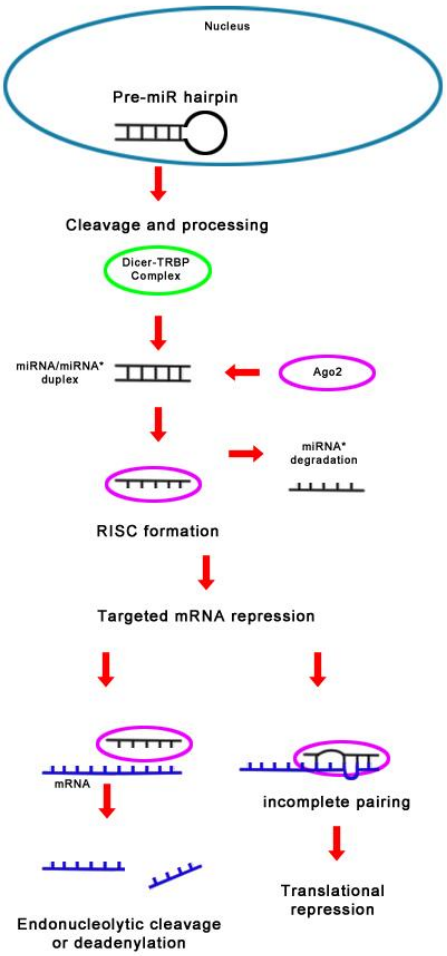

Fig. 4 - microRNA biogenesis and function
The precursor miRNA goes through several steps of processing before assembling into miRISC and targeting mRNA to silence expression by translational repression or destabilization.

Studies on miRNAs have made it apparent that certain miRNAs were highly conserved and expressed in specific tissues[30]. A family of muscle-specific miRNAs was identified by Sempere et al. when they observed miR-1, miR-133a, and miR-206 in striated muscle cells[31]. These were coined 'MyomiRs' and later expanded to include miR-208a, 208b, miR-499 and miR-486[30]. These MyomiRs are of especial interest in this study because of their possible role during biomechanical induction of VSMC differentiation. Other miRNAs have been implicated in myogenesis of smooth muscles, such as miRNA-27 (miR-27). miR-27 is upregulated in cases of

pulsatile shear stress in the blood vessels and also in endothelial cells and highly vascularized tissues[32]. While miR-27 can have multiple targets, PAX3, a skeletal muscle SC regulator, is one that is known to antagonize skeletal muscle differentiation and promote MYOCD[33, 34]. miR-143/145 have also been found promote the MYOCD/SRF pathway, such that miR-145 is considered a phenotypic marker for VSMCs[35, 36]. These miRNA and their relation to shape induced differentiation will be carefully considered in this study.

1.7 Hypothesis and specific aims

Objective: In this study, the effects of shape anisotropy on the differentiation of MSCs to vascular smooth muscle cells (VSMCs) are investigated. The molecular mechanism is delineated by profiling the changes in miRNAs and their downstream genes. Currently, in vitro differentiation protocols of VSMC from MSCs and embryonic stem cells (ESCs) are imperfect, leading to VSMC-like cells with increased phenotypic markers of VSMCs. The results of this study will aid in the development of standardized SMC differentiation protocols, improving the *in vitro* VSMC cultures for drug testing and modeling applications, as well as increasing our understanding of the underlying pathways that link cell environment and function. It may also lead to advancements in regenerative medicine and miRNA therapeutics relating to vascular growth and pathological dedifferentiation in VSMCs.

Hypothesis: I hypothesize that mechanical cues can work in conjunction with biochemical stimuli to help determine the differentiation of MSCs towards VSMCs. Furthermore, I propose that miR-27 and 145 exert important silencing actions that help dictate SMC differentiation. By modulating the actions of miR-27 and 145, I aim to control the synergistic effects of biochemical and biomechanical signaling to push MSCs towards the VSMC phenotype.

Specific aim 1: Characterize the synergistic effect of cell shape elongation and TGF-β in inducing human MSC towards the contractile VSMC phenotype through human MSC culture on micropatterned PDMS scaffolds

The study was performed on human MSCs by seeding cells on micropatterned gel scaffolds with straight microgroove channels of 50 μm, 25 μm, and 10 μm widths, as well as a flat control. The cells were cultured in Dulbecco's modified Eagle's medium (DMEM) with and

without TGF-β. These gels were fabricated with soft lithography techniques. The MSCs were characterized for their SMC phenotypes using Western blot, RT-qPCR, and fluorescence microscopy. SM-actin-α (SMA), SM22-α (SM22), myosin heavy chain 11 (MYH11), and calponin (CNN1) were assayed as these genes have been shown to be key markers of contractile VSMCs[37]. Fluorescence microscopy was performed to directly visualize contractile protein structures.

Specific aim 2: Identify post transcriptional regulators (viz. miRNAs) of induction of VSMC differentiation by shape anisotropy

MSCs were seeded on flat and 10-μm wide microgroove gels and cultured with TGF-β for 3 days. Thereafter, the cells were subject to profiling by miRNA RT-qPCR to determine the effects of the microgrooves on miR-1, 27a, 27b, 133, 143, 145, 155, 206 and 208, all of which have been implicated in events related to vascular proliferation and differentiation[30, 32, 33, 35, 38, 39]. Potential muscle specific regulators were selected based on the effects microgrooves on their expression. The direct effect of miRNA regulation was validated through transfection in gain-of-function and loss-of-function experiments.

Specific aim 3: Evaluate the mechanical phenotype of the microgroove-cultured MSCs and assess their functionality as smooth muscle cells

Using cell traction force microscopy (CTFM), differences in the contractile force generated by the microgroove-cultured MSCs were quantified as compared to MSCs cultured on flat gels, as well as primary smooth muscle cells. These experiments also served to validate the roles of the miRNA regulators by the gain-of-function and loss-of-function experiments.

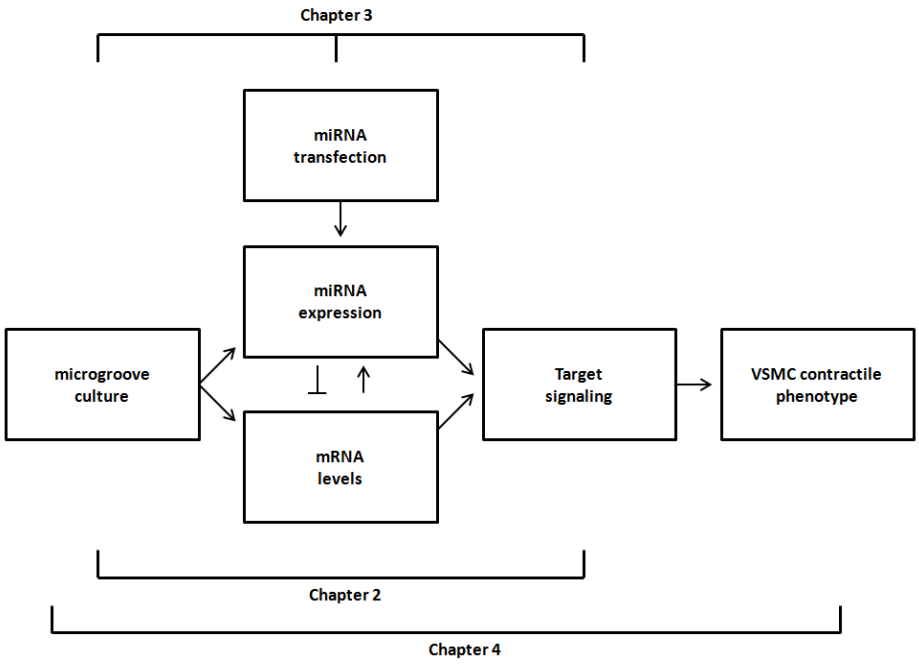

Fig. 5 - Overview of experimental design
In vitro experiments focus on validating VSMC phenotypic markers as a result of microgroove culture in Chapter 2. Chapter 3 identifies miRNA roles in induction by shape anisotropy and Chapter 4 evaluates functional regulation through miRNA validated in Chapter 3.

1.8 Broader impacts

This research could help to advance the use of miRNA as a therapeutic target by showing its integral role in vascular development. Advancing knowledge of SMC differentiation in the context of miRNA will also allow for the generation of sustainable and more cost-effective SMC sources for vascular tissue modeling and possibly even tissue constructs for patients who need transplants by use of autologous cells. Commercialization of SC derived vascular tissue implants would be medically valuable as the number of patients waiting for donors continues to rise.

CHAPTER 2. VSMC DIFFERENTIATION INDUCED BY CELL MORPHOLOGY MODULATION THROUGH CULTURE ON MICROGROOVE SUBSTRATES

2.1 Abstract

Biomechanical effects play important roles in regulating the development of VSMCs that are difficult to explain fully. The morphological changes that accompany phenotypic changes during SMC transition between functional phases suggest cell shape as a particular property to consider. Cell-shape regulation of VSMCs has been shown to regulate proliferation and induce contractile phenotype[25, 40]. In order to validate the differentiating effect of cell morphology on MSCs, I designed a study that allows for precise manipulation of the microenvironment with the proper controls. Soft lithography provides a platform through which polymer-based microgroove substrates can be constructed with precise control of the width of the cells. This would drive the MSCs towards the VSMC lineage such that phenotypic gene expression can be detected in the microgroove-cultured MSCs. The aim was to provide novel insights on the role of mechanotransduction in VSMC differentiation.

2.2 Bioengineering problem definition and analysis

Problem Definition and Engineering Considerations

My goal is to better understand the mechanisms by which MSCs respond to geometrical cues in the context of miRNA pathways. Thus, I designed and constructed an appropriate seeding platform that modulates the shape of the cell while keeping other parameters constant. The following questions were considered: (1) What cell line to model? (2) What are the parameters of the platform for cell seeding? (3) How will the cells be cultured and the culture conditions modulated? and (4) How will the outcome be determined?

Design Criteria for Engineering Considerations and Proposed Solutions

MSCs are a multipotent stromal cell type that is a precursor to VSMCs, making it a prime model to work with to study induction of the SM pathway by shape modulation. Using human MSCs ensured the results of this study to be relevant to vascular diseases and developing regenerative technologies. I considered this a proper justification for the increased cost to use the human cell model for this study. Also, with current trends in research leaning heavily towards regenerative medicine, I believe further advances in the human model is well timed to help advance vascular related therapies.

Foremost, the design of the culture substrate must allow for the control of surface topography, cell spreading, and cell morphology. To accomplish these, microfabrication through soft lithography was employed. I decided to fabricate the substrate on polydimethylsiloxane (PDMS) for its low cost, ease of use, and biocompatibility. The advantageous properties of PDMS have led to its widespread application in soft lithography, as well as other biomedical applications such as microfluidics and bioMEMS[41]. The substrate surface is designed to restrict cell growth in the perpendicular direction by a parallel microgroove pattern. The channels and walls are of equal width with variations at 25, 50, and 10 μm (Fig. 6). All wall height was set at 5 μm as the increasing the height further would decrease the stability of the micropatterned features. The gels were 2 cm x 3 cm x 0.2 cm which allowed them to fit in a standard 60 x 15 mm Petri dish to facilitate storage, transport and culturing. In my *in vitro* cultures, the MSCs reached ~90% confluent at 1-3 x 10^4 cells/cm^2 [42]. To seed the gels to confluency, the gel surface area was calculated as ½ the apparent surface area since at the microscale the walls and the grooves each occupied one-half of the surface. Thus, assuming 2 x 10^4 cells/cm^2 at confluence, optimal seeding density on the gels was ~6 x 10^4 cells/cm^2. This created a relatively even seeding of the microgroove substrates as the cells tended to adhere inside the microgroove channels.

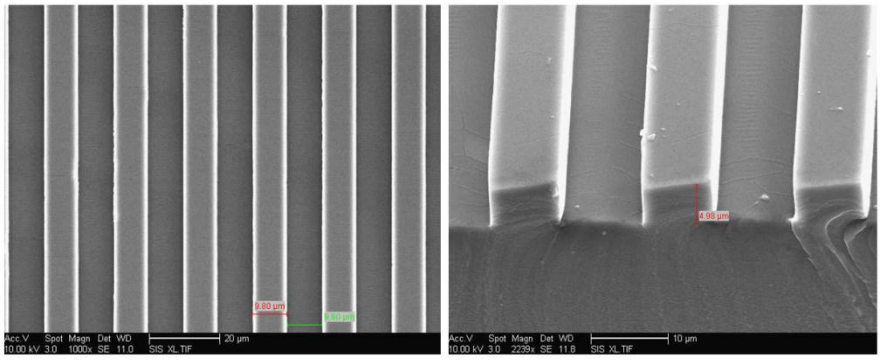

Fig. 6 - 10-µm width PDMS microgrooves
These images taken by scanning electron microscopy (SEM, showing an aerial view (left) and angled view (right) of the 10-µm wide PDMS microgrooves.

2.3 Materials and methods

2.3.1 Cell culture

Human bone marrow-derived mesenchymal stem cells (Cell Applications) were cultured in 100- mm cell culture dishes and maintained in human marrow stromal cell growth medium (Cell Applications). They were passaged once the cells reached 80-90% confluency. MSCs within passages 5-8 were used in all experiments.

2.3.2 PDMS microgroove fabrication by soft lithography

A silicon wafer was prebaked for 5 minutes at 95°C before plasma etching the surface by using a Technics PEIIB planar etcher. Photoresist (SU-8 2005) was spin-coated onto the wafer to desired thickness and soft baked at 95°C for 2 minutes. The wafer was exposed to ultraviolet light for 2.5 seconds using a photomask patterned with our 10-µm channels using the Karl Suss MA6 Mask Aligner. After hard baking at 95°C for 3 minutes, the UV cross-linked the UV-exposed photoresist . The wafer was then washed in SU-8 developer for 1 minute and followed by IPA for 1 minute. To wash out the unpolymerized photoresist completely, the silicon wafer was rinsed with ddH_20 and then air dried. PDMS (Sylgard 184) was then mixed at 10:1 ratio with PDMS

curing agent and poured over the patterned wafer mold to form the features. The PDMS was cured for 1 hour at 60°C before it was peeled off and sectioned into individual gels. The gel surfaces were treated by plasma etching by Technics PEIIB planar etcher for 7 minutes to improve surface hydrophilicity.

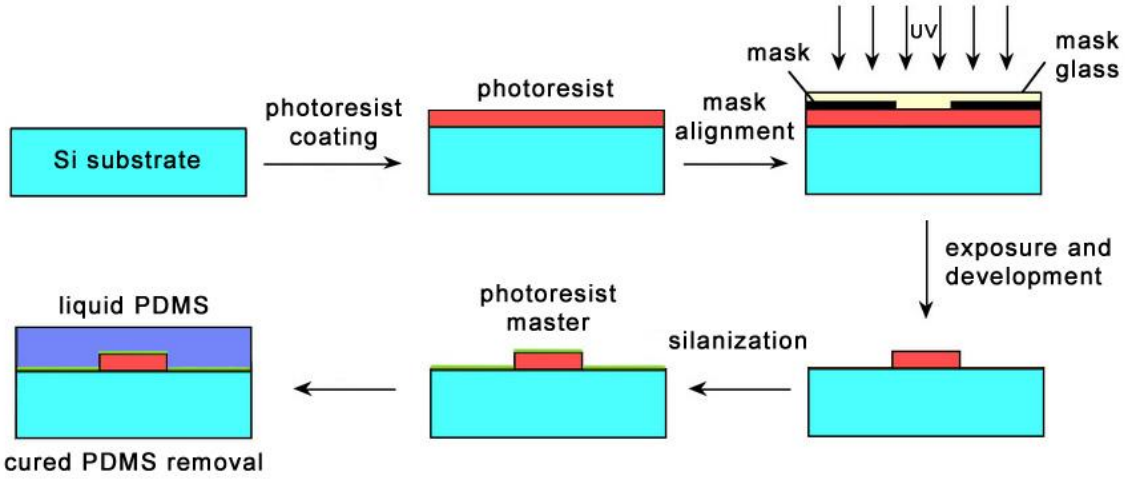

Fig. 7 - Soft lithography microgroove fabrication procedure
Photoresist (SU-8) was spin-coated onto a silicon wafer to desired thickness and exposed to ultraviolet light using a photomask patterned with our 10-µm channels. The UV cross-linked the exposed photoresist and, after development, the unpolymerized photoresist was washed off of the silicon wafer. PDMS (Sylgard 184) was then prepared and poured onto the patterned mold to form the features.

2.3.3 Microgroove culture conditions

The PDMS gels were coated with fibronectin (50 ng/µl) and stored at 4°C overnight before seeding. MSCs were seeded onto the PDMS gels at ~$1x10^4$ cells/cm^2. The seeded cells were then cultured for 3 days in DMEM with 10% fetal bovine serum (Omega Scientific), 1% penicillin-streptomycin (Thermo Fisher), 1% 100mM sodium pyruvate (Thermo Fisher), and 1% 200 mM L-Glutamine(Thermo Fisher) supplemented with 5 µg/ml TGF-β (Peprotech).

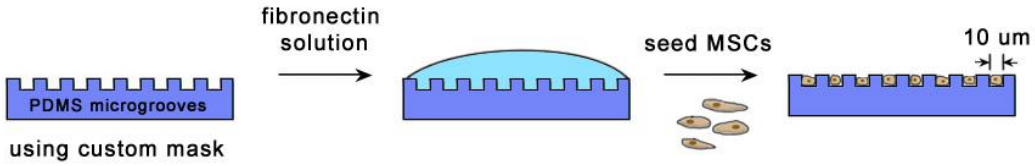

Fig. 8 - Seeding of PDMS microgrooves
The PDMS microgrooves allowed us to modulate cell geometry and shape by seeding the cells into the thin channels. The PDMS was coated with fibronectin solution at 50 µg/ml to allow the MSCs to attach.

2.3.4 Statistical analysis

All data are represented as mean ± standard error of the mean (SEM) and compared among separate experimental groups. Student's t-test was used to determine the level of significance between two groups. P values <0.05 were considered as statistically significant.

2.3.5 Western blot

MSCs were lysed with radio immunoprecipitation assay (RIPA) buffer. Protein lysates were centrifuged to remove cell debris, and the supernatant was separated and quantified by Bio-Rad Protein Assay. Protein samples, along with Bio-Rad rainbow protein molecular weight marker, were run using 10-well sodium dodecyl sulfate-poly acrylamide gel electrophoresis (SDS-PAGE). Proteins were transferred onto nitrocellulose (NC) membranes and blocked with 5% BSA. Membranes were then incubated with primary antibodies at 1:1000 dilution overnight and 4°C. Primary antibodies included MYH11, SMA, CNN1, SM22 and GAPDH. Next day, NC membranes were washed 3 times for 10 minutes each, using 0.1% tris-buffered saline and tween-20 (TBST); correlating secondary antibodies coupled with horseradish peroxidase (Santa Cruz Biotech) were added and incubated for one hour at room temperature. Using the enhanced chemiluminescence (ECL) detection system (Thermo Fisher), the bound primary antibodies on NC membrane were imaged then quantified using ImageJ.

2.3.6 RNA isolation

Growth media was removed from the culture dish with the cells seeded on the PDMS substrate. Cells were lysed directly using 1mL of TRIzol reagent (Thermo Fisher) and stored in -80°C until ready for processing. The samples were thawed and incubated for 5 minutes at room temperature before adding 0.2 mL of chloroform. The samples were incubated at room temperature for another 3 minutes before centrifugation at 12,000 g for 15 minutes at 4°C. The aqueous phase was pipetted into a separate tube and mixed with 0.5 mL of 100% isopropanol. The sample was incubated for 10 minutes at room temperature before centrifugation at 12,000 g for 10 minutes at 4°C. Thereafter, the supernatant was discarded and the RNA pellet was washed with 1 mL of 75% ethanol. The sample was centrifuged at 7,500 g for 5 minutes at 4°C. The supernatant was discarded and the pellet was air-dried for 15-20 minutes. The pellet was then resuspended in 20 µL of nuclease-free water and measured for total RNA concentration using the NanoDrop 2000c (Thermo Scientific).

2.3.7 RT-qPCR

Reverse transcription (RT) was performed using oligo(dT) to produce cDNA. Quantitative polymerase chain reaction (qPCR) was performed with custom primers from Applied Biosystems for specific miRNA detection. qPCR was performed using real-time qPCR machine (Bio-Rad) following the manufacturer-suggested protocol. In general, three or more biological replicates were used for statistical analysis and reactions were run in duplicate to ensure accuracy of the TaqMan primers. RNU48 was used as the internal control to determine relative expression levels of miRNAs.

2.3.8 Cell morphology characterization

To compare the morphological changes of MSCs as a result of microgroove culturing, the cells were seeded on both nonpatterned flat gels and microgrooves with varying widths (50,

25, and 10 µm). After 3 days, phalloidin staining revealed F-actin fiber bundles and their orientation. DAPI staining was used to visualize the cell nuclei. To quantify the microgroove effect on cell morphology, the cell area and shape index were statistically analyzed using ImageJ. The nucleus area and aspect ratio were also measured.

2.4 Results

2.4.1 PDMS microgrooves promote cell shape anisotropy

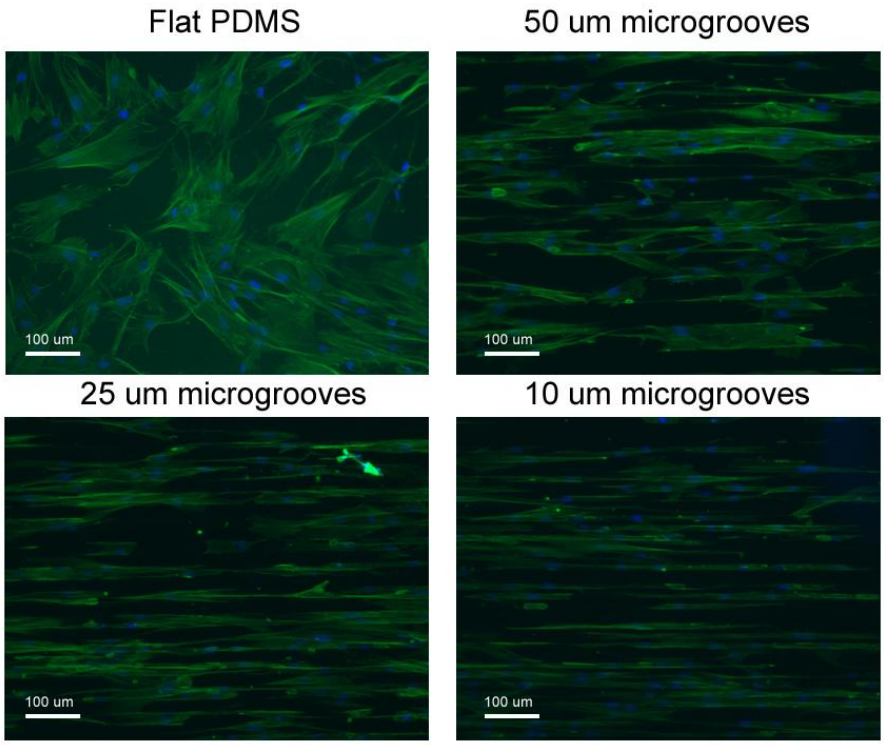

Fig. 9 - Actin stress fiber and nuclear staining on flat and varying microgroove width gels
Fluorescent microscopy images were taken from cells seeded on PDMS gels. The seeded cells naturally settled into the channels and developed an elongated shape. F-actin fibers were stained by phalloidin (green) and nuclei are stained by DAPI (blue) . The procedure was tested on flat, 50-, 25-, and 10-µm microgroove channels.

On the flat gel, the cells spread out into fibroblast-like shape with no orientation of the F-actin structures (Fig. 9). The microgroove-cultured samples showed restricted cell area and elongation of the cells, aligning the cells parallel to the direction of the microgrooves (Fig. 9). As

the channel width of the microgrooves change, the cell width also changed accordingly. When comparing the sample groups, significant differences were most consistently seen between the cells cultured on the flat surface vs those on 10-µm width microgrooves. Nucleus area, cell area, and cell shape index (CSI) were significantly smaller on the 10-µm microgroove MSCs compared to the flat substrate MSCs, indicating that the microgrooves restricted cell spreading in the perpendicular direction and promoted elongated morphology. Since these effects were most pronounced on the 10-µm wide microgrooves, subsequent experiments were conducted with that channel width. Smaller widths (<10 µm) led to the spreading of the cell over the microgroove walls, resulting in a more inconsistent cell width.

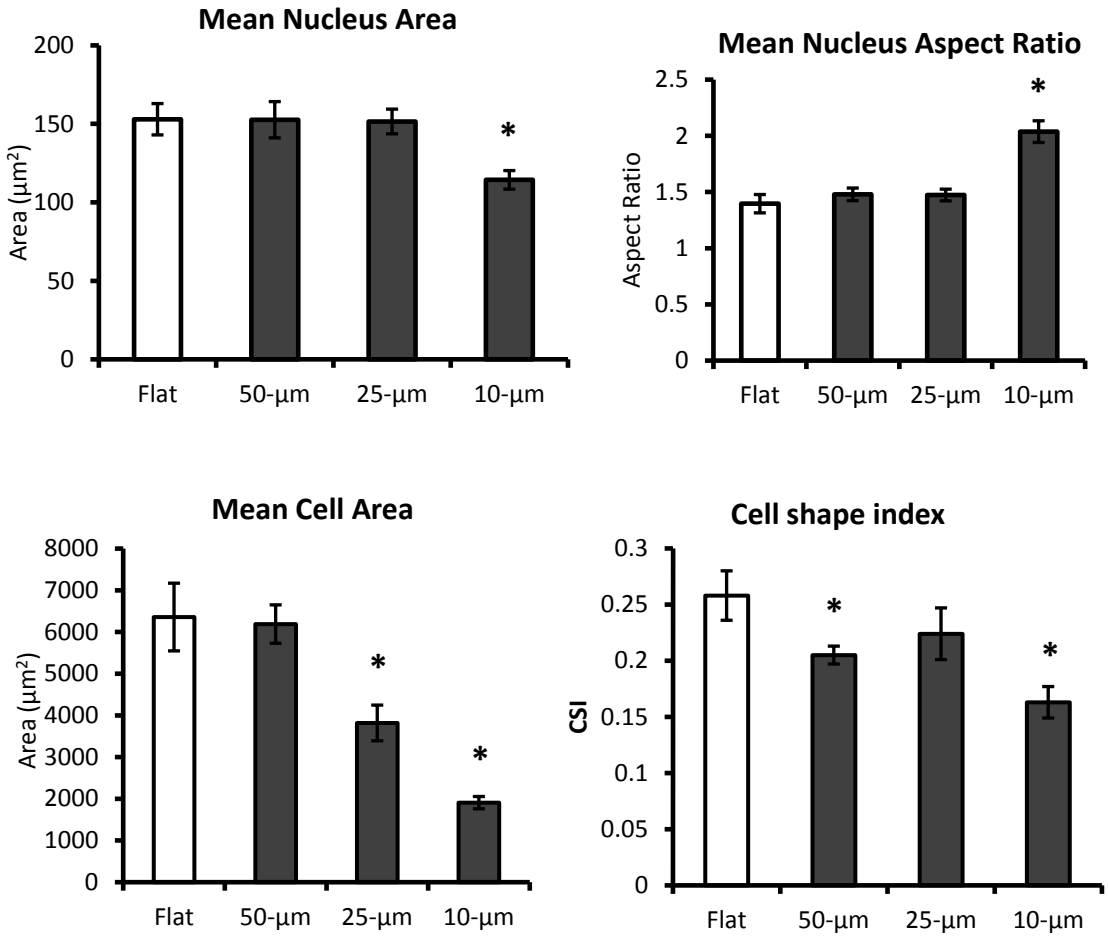

Fig. 10 - Effect of microgrooves on MSC morphology
MSCs seeded on flat PDMS gels or PDMS microgrooves of 50-, 25-, and 10-μm widths over 3 days. Mean nucleus area was obtained by DAPI staining and analysis in ImageJ. Mean nucleus aspect ratio was found by measuring the long and short axes of the nucleus. Cell area was found by F-actin staining. For the cell shape index (CSI), cell area and perimeter were measured to quantify CSI. CSI was defined as $4\pi \times \text{area}/\text{perimeter}^2$.

2.4.2 Microgrooves upregulate smooth muscle-specific phenotypic markers

Having shown the morphological effects of the microgrooves on the MSCs, I investigate the potential for the microgrooves to induce the MSCs to move towards a VSMC phenotype. Fluorescent microscopy of microgroove-cultured MSCs revealed the development of smooth muscle specific α-SMA contractile structures parallel to the microgroove direction (Fig. 11). MSCs cultured on flat substrate did not show significant SMA structures. In order to quantify the effects of the microgrooves compared to flat substrate, a spectrum of phenotypic markers of

VSMCs were selected for protein levels and gene expression profiling of flat and microgroove cultured MSCs. Western blot analysis was performed on protein samples from flat gel and microgroove widths at 50-, 25-, and 10-μm, and RT-qPCR was performed on total RNA samples from flat gel and 10-μm microgrooves as validation. Western blots showed significant increases in VSMC markers SMA and MYH11 in the microgroove cultured MSCs, with a general increasing trend as the width decreased (Fig. 12). SM22 level was highly induced by TGF-β, and was not further induced by microgroove width narrowing (Fig. 12). RT-qPCR results comparing flat and 10-μm microgroove cultures at 3 days also showed significant microgroove-increased levels of SMA and CNN1. However, the increases for MYH11 and SM22 were not statistically significant (Fig. 13), possibly due to the large standard error, or high TGF-β/flat-induced expression as indicated by Western blot results. The results indicate that constricting the cell morphology into an elongated shape promoted certain VSMC phenotypic markers, but did not induce a full VSMC phenotype.

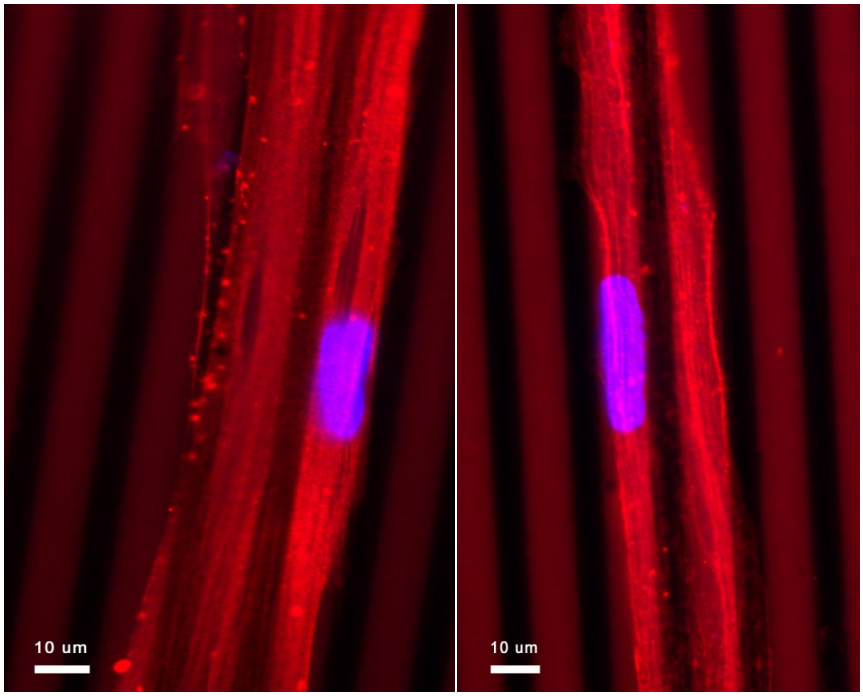

Fig. 11 - 10-µm microgroove MSCs stained for anti-α-SMA
Fluorescent imaging showed microgroove cultured MSCs with the nucleus stained with DAPI (blue) and α-SMA fiber structures stained with anti-α-SMA antibody (red). Contractile α-SMA structures were aligned in the direction of the microgrooves.

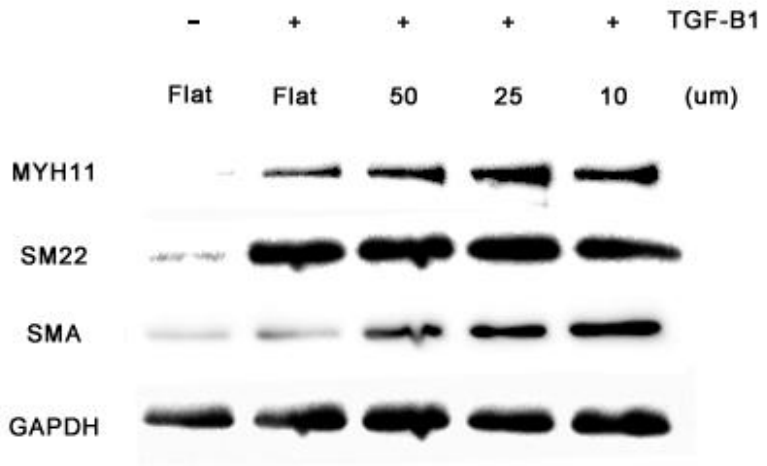

Fig. 12 - VSMC markers across varying width microgroove cultured MSCs
As channel width decreased, the expression of smooth muscle phenotype markers MYH11 and SMA increased. There was no significant change in SM22.

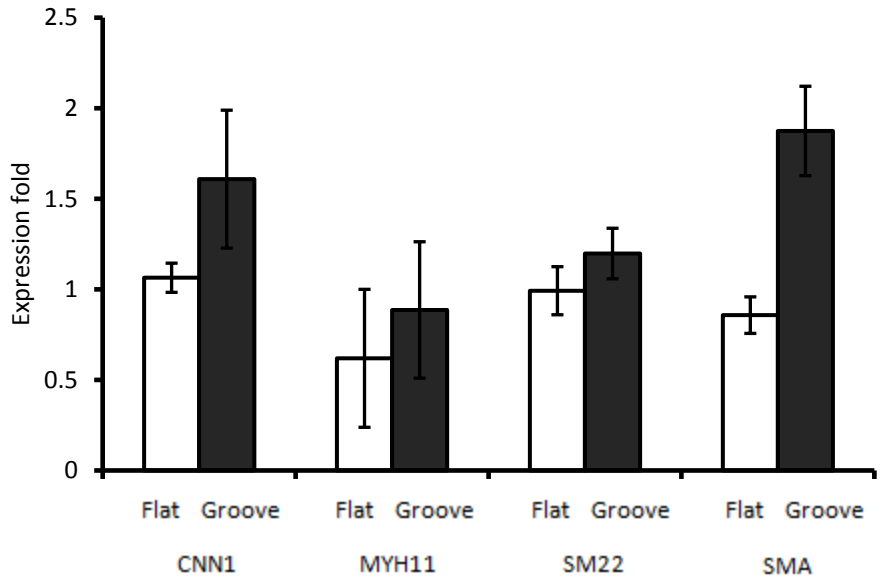

Fig. 13 - RT-qPCR analysis for VSMC markers of 10-µm microgroove cultured MSCs
The RT-qPCR results reflect similar trends as the Western blots, showing significant increase in SM markers such as CNN1 and SMA. Also, SM22 and MYH11 did not show significant change. MSCs were cultured under the same conditions on the 10-µm microgrooves for 3 days.

2.4 Chapter 2 discussion

For this study, soft lithography was used as a fabrication method to provide the geometric control over the substrate topography. SEM and light microscopy were used to examine the features and ensure proper manufacturing. Images of MSCs revealed that the microgrooves could restrict and align the cell shape and direction, introducing a mechanical stimulus to the cell culture. While the mechanism of transducing the shape modulation remains unclear, the microgrooves induced morphological changes in both the cell and the nucleus. It also restricts the deployment of the focal adhesions, forcing them to align along the groove. These findings indicate that cell spreading was severely limited by the microgrooves. While the mean cell area decreased, no conclusion can be drawn on the cell volume due to lack of information on cell height. Future study with fluorescent z-stack of images can be used to verify whether microgrooves have any effect on cell volume.

The microgroove PDMS substrate was applied as an *in vitro* model to identify geometrical cues that induce the differentiation of MSCs to VSMCs. Culture of MSCs on PDMS microgrooves showed increases of SM-specific markers SMA, MYH11, and SM22 in Western blot. RT-qPCR showed significant increases in SMA and CNN1. The results suggest that, among the SM markers analyzed, SMA responded the most to the cell shape induction of SM gene expression, while the results on MYH11 and CNN1 were less consistent between Western blot and qPCR. SMA in particular shows clear development in the formation of contractile protein structures, aligning parallel to the microgroove direction (Fig. 11). Thus, the modulation of the morphological state of MSCs by the microgrooves resulted in phenotypic transitions. This transition is relevant to the morphological differences between elongated, contractile VSMCs and rhomboid, synthetic VSMCs. Since the contractile, functional phase of the VSMCs presents a spindle shape, the elongation of the MSCs may in turn facilitate transition into contractile VSMCs.

As a caveat to the results, while the experiment is well suited to gauging the isolated effects of cell shape alone, I cannot say that the PDMS microgrooves accurately mimic the *in vivo* microenvironment. The PDMS used is stiffer than the vascular tissue, and making the gel softer risks the structural integrity of the substrate features. Also, separation of the cells by the microgrooves removed cell-cell interactions. Other studies have used shallower, ridged topographies instead of microgroove channels, aligning the cells through contact guidance[40]. This allows cell-cell interaction and the ability to seed at high confluence. However, the design used in this study allows for a stricter control of the cell width. Other studies have used softer polymers such as polyacrylamide and to pattern an ECM protein such as fibronectin or collagen to restrict cell seeding along a line. However, this is more akin to restricting cell spreading rather than controlling cell shape, and it is difficult to say whether the effect would be the same on the

MSCs. Given that my design may have reduced the number of other factors influencing the cell, the microgroove substrate could be justified, but further studies are needed to explore other means of modulating cell morphology.

In my preliminary studies on similar experiments conducted without the presence of TGF-β in the culture media, the 10-μm microgrooves led to slight, but insignificant changes in VSMC marker expression. Supplementing the growth media with TGF-β in both the control and microgroove cultures increased the relative difference in marker expression, suggesting that the microgrooves alone are not sufficient to differentiate the MSCs. However, they may amplify or facilitate the differentiation effects, steering the cells more towards the VSMC lineage. It is known that TGF-β plays an important role in cell differentiation, and is able to induce morphological changes and actin fiber synthesis in MSCs[12]. The finding that the microgrooves enhanced assembly of SMA and other SM markers confirms that the cell shape mechanotransduction is related to the TGF-β family pathway and MSC differentiation. However, the nature of the mechanism itself requires further studies. In order to identify key regulators that mediate the microgroove-induced differentiation, genomic profiling and validation were performed for the myogenesis-related miRNA, and these studies are presented in the following chapter.

CHAPTER 3. miRNA AS POST-TRANSCRIPTIONAL REGULATORS FOR MICROGROOVE-INDUCED VSMC DIFFERENTIATION

3.1 Abstract

Chapter 2 presents the mechanical induction of VSMC differentiation by cell shape manipulation. The studies in this Chapter 3 aims at elucidating the underlying mechanism by identifying the post-transcription regulators that mediate the microgroove-induced differentiation. miRNA provides a promising therapeutic approach with its regulatory mechanism operating through sequence-specific binding to silence mRNA expression. The exact target or set of targets for a given miRNA is often difficult to identify, making the full extent of their effects unclear. However, growing evidence has indicated that they play critical roles in vascular homeostasis and development[43-45]. In order to assess the roles of miRNA in microgroove-induced differentiation, the microgroove-cultured MSCs were profiled for miRNA related to myogenic regulation. I found that miR-27 and miR-145 showed significant responses to microgroove culture, with miR-27 being downregulated and miR-145 being upregulated after a 3-day trial. Gain-of-function and loss-of-function experiments were conducted to determine whether downregulation or upregulation of miR-27 and miR-145 could modulate the effect on VSMC differentiation by microgroove culture. The results indicate that miR-27 and miR-145 play repressive and promotive roles, respectively, in the microgroove-induced VSMC differentiation.

3. 2 Introduction

In order to assess the role of miRNAs as regulators in microgroove-induced MSC-to-VSMC differentiation, the RNA isolated from microgroove-cultured MSCs were profiled for the expressions of miR-1, 27ab, 133a, 143, 145, 155, 206, and 208. Each of them has been previously implicated in the myogenic process, though most have not been linked to mechanotransduction.

For miR-27, it has been previously shown that the neonate muscle in developing swine skeletal cells has a ten-fold reduction as compared to the satellite cells[46]. It has also been shown that miR-27 is instrumental in the promotion of osteoblast differentiation via the activation of Wnt signaling through β-catenin accumulation[47]. MyomiRs such as miR-1, miR-133, and miR-206 have been shown to be significantly upregulated during myogenesis[48, 49]. Others like miR-208 and miR-499 have been linked to muscle atrophy, the downregulation of which leads to repression of the β-MHC gene, an indicative sign of the pathology[50]. miRNAs may produce opposite effects; for example, Angiotensin II (Ang II) has been found to be indirectly upregulated by miR-143/145 while downregulated by miR-155[39, 51]. Ang II is a vasopressive agonist of VSMC contraction as well as a major regulator of the contractile phenotype that is linked to pathophsiological thickening of vasculature [52, 53]. miR 143 and 145 are of particular importance due to their role in the MYOCD/SRF pathway, a major inducer of the contractile phenotype[35]. miR-145 has been found to exist at high levels in VSMCs *in vivo*, and is considered a VSMC phenotypic marker[36]. Its expression mirrors closely other marker genes such as SMA, CNN1, and MYH11, and is reduced significantly after angioplasty, reflecting the VSMC dedifferentiation [36]. Thus, myomiRs play a role in numerous cellular processes in VSMCs, including cell fate, proliferation, plasticity and pathological progression. Genomic profiling for this set of miRNA may yield new insights on the post-transcription regulation of VSMC differentiation in response to geometric cues. This study also points out possible therapeutic targets among these miRNA for the regulation of SMA phenotype to alleviate conditions such as atherosclerotic lesion progression and restenosis.

3.3 Materials and methods

3.3.1 Transfection

Antagomirs and precursor miRNAs (Ambion) were used in the gain-of-function and loss-of-function experiments, along with the respective negative control molecules. The oligonucleotides were reverse-transfected in separate wells of a 6-well plate using Lipofectamine 2000 (Thermo Fisher) in 2 mL of Opti-MEM (Thermo Fisher). The final concentration of the transfection molecules was 100 nM.

3.3.2 Microgroove fabrication and cell culture

See sections 2.3.1-2.3.3. The width of microgroove substrates for all the experiments conducted in this chapter is 10 μm.

3.3.3 Isolation of small RNA molecules

Small RNA was iolated using the mirVana miRNA Isolation Kit (Thermo Fisher). The cells were lysed using 400 μL of lysis binding solution followed by 1/10 volume of miRNA homogenate additive. The samples were incubated on ice for 10 minutes before the addition an equivalent volume of acid-phenol:chloroform. The entire mixture was vortexed and centrifuged at 10,000x g at room temperature for 5 minute. The aqueous phase was pipetted into a separate tube, and 1.25 volumes of 100% ethanol was added. This solution was transferred into the RNA binding column and centrifuged at 10,000x g at room temperature for 15 seconds. The column was then washed once with 700 μL of wash solution 1, followed by 500 μL of wash solution 2/3 twice. The filter was centrifuged for an additional minute before transferring into a new collection tube. Finally, 50 μL of nuclease-free water heated to 95 °C was added to the filter cartridge to collect the miRNA by centrifugation for 30 seconds.

3.3.4 miR RT-qPCR

Reverse transcription (RT) and quantitative polymerase chain reaction (qPCR) were performed with TaqMan miRNA assays (Applied Biosystems) with specific miRNA primer sets. qPCR was performed using a real-time PCR machine (Biorad) following the protocol suggested by the manufacturer. Three or more biological replicates were performed for statistic analysis, and the reactions were run in duplicates to ensure the accuracy. RNU48 was used as the internal control to determine the relative expression levels of miRNAs.

3.4 Results

3.4.1 Profiling of myogenesis-related miRNA in MSCs cultured on microgroove substrate reveals miR-27 and miR-145 as potential regulators

After 3 days of culture on the microgroove substrate, miR-145 was significantly increased in MSCs compared to MSCs cultured on flat substrates (Fig. 8), while miR-27a and b were significantly decreased. The two isotypes of miR-27 were probed separately despite having identical seed sequences, since the nature of incomplete miRNA pairing does not guarantee that they share the same targets. While miR-208 did show a significant increase in expression, its relatively high PCR cycle numbers suggested a low expression level. Since this has the risk of false positive results, miR-208 was not included for further study. Other miRNAs profiled did not show significant changes over the same time course. miR-1 was also excluded from the data due to low expression level, which led to large variations among the samples. The overall results suggest that miR-27 and miR145 may play a role in regulating MSC differentiation towards the contractile VSMC phenotype. To validate their roles in the shape-induction of VSMC differentiation, gain-of-function and loss-of-function experiments were then performed by

transfection of silencing and promoting miRNA molecules into MSCs cultured on flat and microgroove substrates.

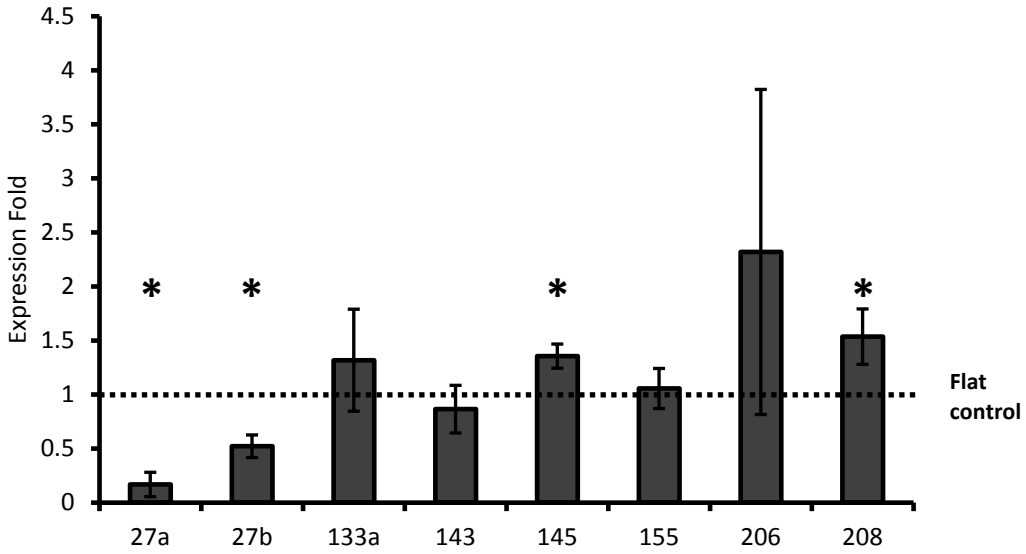

Fig. 14 - Effects of microgrooves on myogenesis-related miRNA expression levels after 3 days
To further characterize how cell shape modulation regulates VSMC differentiation, the expression levels of selected miRNA known to regulate VSMC functions were profiled with miRNA TaqMAN RT-qPCR. The results were normalized to the internal control (RNU48). Microgroove culture caused the significant downregulation of miR-27ab and upregulation of miR-145 and miR-208. * Asterisks denote statistical significance ($P<0.05$)

3.4.2 Gain-of-function and loss-of-function experiments for miR-27 and miR-145

The results of the microgroove-regulation of miR expression (Fig. 14) suggest that miR-27 may play a repressive role, while miR-145 may be promotive, in regulating MSC differentiation. Having identified these potential regulators, I transfected anti-miRs and pre-miRs of mIR-27 and -145 into MSCs before culturing them on the microgroove and flat substrates. It was expected that anti-miR-27 and pre-miR-145 would help induce the transition to the VSMC phenotype while pre-miR-27 and anti-miR-145 would inhibit it. The gain-of-function and loss-of-function experiments for miR27 were designed as depicted in Fig. 15: pre-miR-27 was used for lost-of function, while anti-miR27 for gain-of function, experiments. The experiments were designed similarly for miR-145, with the notable difference that pre-miR-145 was used for gain-of-function and anti-miR-145 was used for loss-of-function. Both flat and

microgroove substrates were seeded with transfected cells of either control molecules, anti-miR-27, anti-miR-145, pre-miR-27 or pre-miR-145. The effectiveness of the transfection molecules was validated by miRNA RT-qPCR, and the expressions of marker genes.

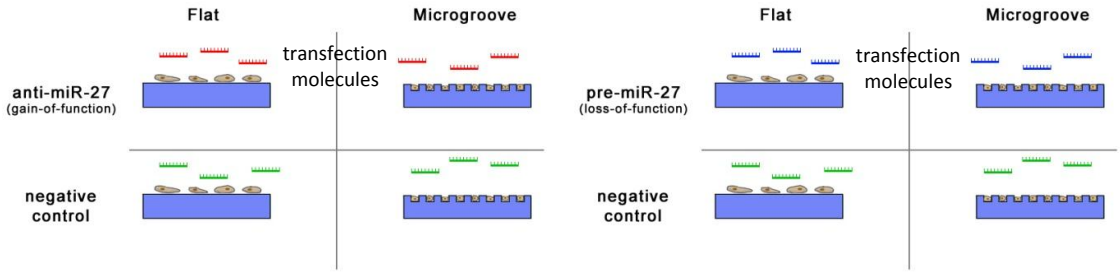

Fig. 15 - Design for gain-of-function and loss-of-function experiments for miR-27
In the gain-of-function experiments (left), MSCs were transfected with miR-27 silencing anti-miRs using lipofectamine. The cells were seeded on 10-μm grooved gels and flat substrates along with a set transfected with a non-targeting negative control. The loss-of-function experiments were prepared similarly with pre-miR-27 transfected instead. After 3 days, the cells were lysed and profiled for VSMC markers by RT-qPCR and Western blot.

The Western blot results showed that SMA and SM22 were upregulated on the microgroove substrate compared to the flat substrate (Fig 16). In gain-of-function experiments, anti-miR-27 and pre-miR-145 caused the upregulation of SM markers such as SM22 and SMA when compared with the flat substrate controls. It is notable that the anti-miR-27 and pre-miR-145 caused a minor elevation of SM marker expression in MSCs cultured on flat substrates, and did not further enhance the SM markers when combined with the microgroove substrate. For example, SMA does not increase on microgroove anti-miR-27 compared to microgroove control as well as flat anti-miR-27. This can also be seen in microgroove pre-145 for both SMA and SM22, suggesting that the gain-of-function transfection did not increase SM markers further when cultured on microgrooves. It is only on flat substrate that a significant increase of SM markers can be seen due to gain-of-function transfection. In the loss-of-function columns, transfections of pre-miR-27 and anti-miR-145 tend to decrease SM marker expression and attenuate the microgroove-induced SM marker expression. These results indicate that miR-27 and miR-145 play significant roles in regulating MSC-SMC differentiation.

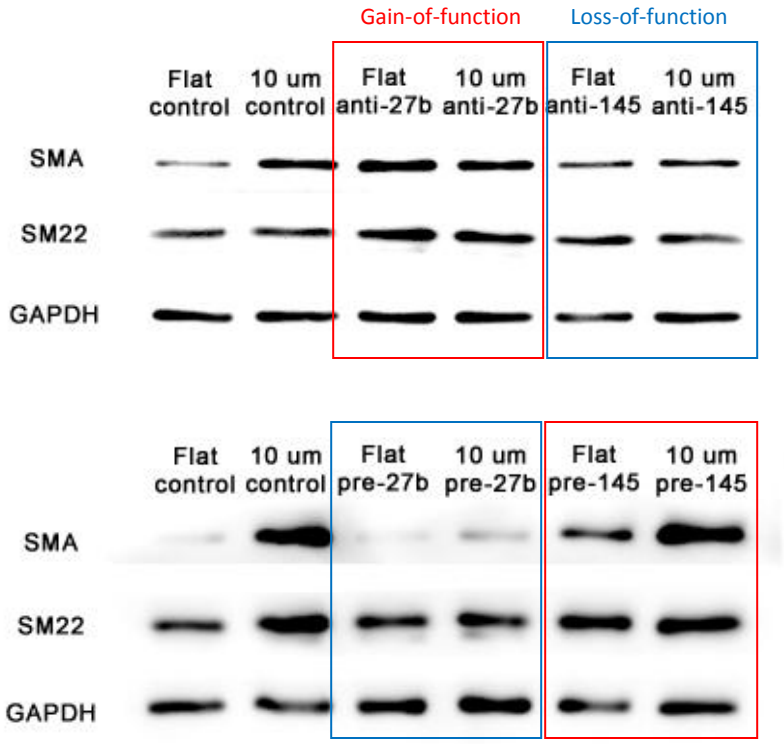

Fig. 16 - Western blots of miRNA-transfected MSCs cultured on flat and microgroove substrates
Gain-of-function results are boxed in red while loss-of-function results are boxed in blue. Across the two Western blots, SMA and SM22 were upregulated in the microgroove control compared to flat control. Addition of pre-miR-145 and anti-miR-27b increased SMA and SM22 in the flat samples, resembling results for the microgroove control. Conversely pre-miR-27b and anti-miR-145 decreased SMA and SM22 in the transfected microgroove samples.

Similar experiments were conducted for RT-qPCR (Figs. 17 and 18). MSCs transfected with control molecules were seeded on flat and microgroove substrates for 3 days. These were compared with MSCs transfected with anti-miR-27 and pre-miR-145 seeded on flat substrate for the gain-of-function experiment, as well as MSCs transfected with pre-miR-27 and anti-miR-145 seeded on microgrooves for the loss-of-function experiment. The samples were probed for SM markers SMA, SM22, CNN1, and MYH11. The gain-of-function results indicate that microgroove substrate and the transfections for anti-miR-27 and pre-miR-145 upregulated the SM markers, with the exceptions that microgroove alone did not induce a significant MYH11 expression, and that anti-miR-27 did not significantly upregulate CNN1.

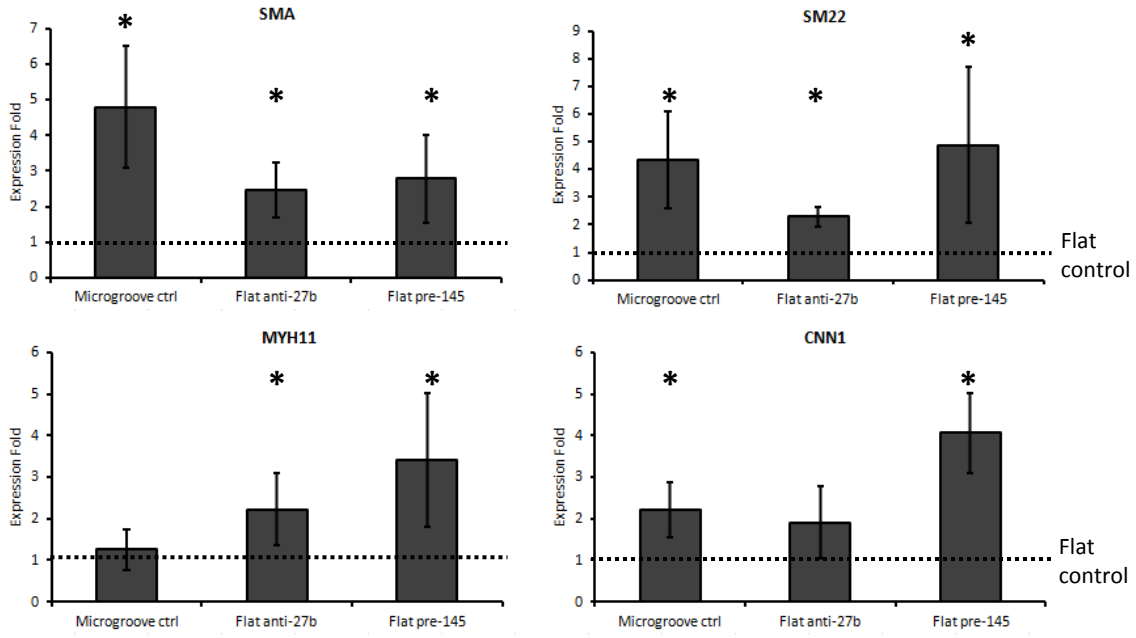

Fig. 17 - RT-qPCR results for gain-of-function experiments
Each of the gain-of-function samples shows general trend of upregulated expression of SM markers SMA, SM22, MYH11 and CNN1 in comparison with flat control. Expression levels are generally above the normalized control baseline expression. MYH11 was not significantly changed by microgroove culture. Asterisks denote significant difference from flat control ($p<0.05$).

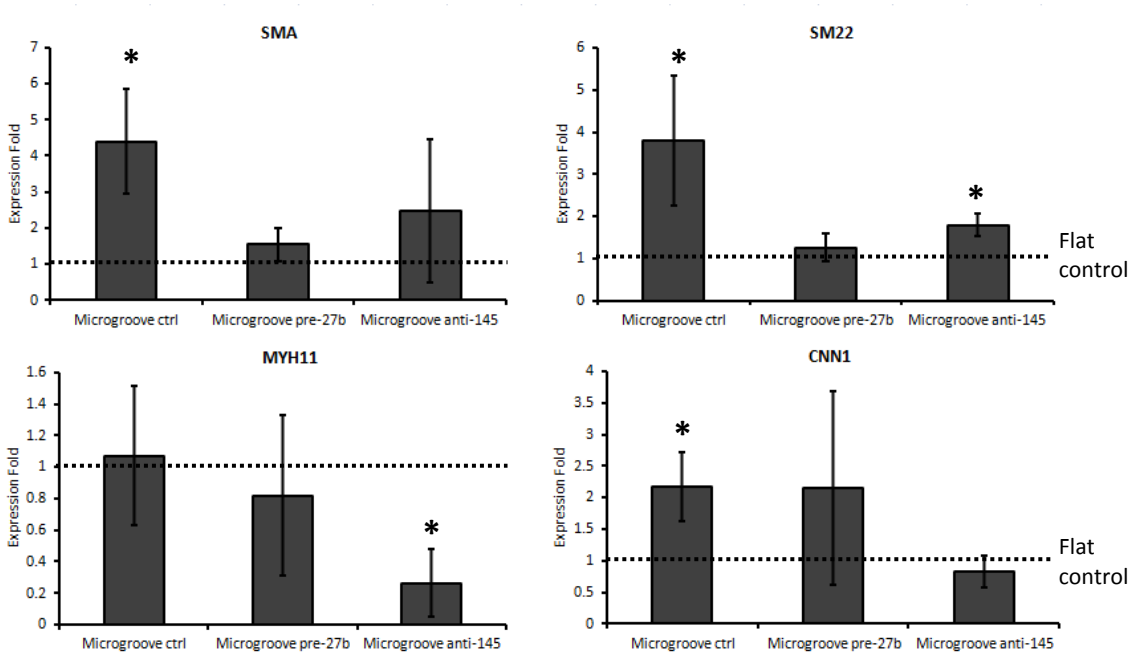

Fig 18. RT-qPCR results for loss-of-function experiments
Pre-27b transfected microgroove samples do not show significant difference from the control baseline expression. Anti-145 transfected microgroove samples showed an increase in SM22 and a decrease in MYH11 as compared with the control baseline. The results suggest an overall attenuation of the microgroove effects by the transfection of pre-miR-27 and anti-miR-145. Asterisks denote significant difference from flat control ($p<0.05$).

In the loss-of-function results (Fig. 18), microgrooves again significantly increased SM marker expression except for MYH11. Transfection of pre-miR-27 and anti-miR-145 resulted in significant decreases of microgroove-induced SM expression; these SM makers were not significantly greater than their expression in cells on the flat control substrates, except for the microgroove/anti-miR-145 treatment on SM22, which still has a markedly lower expression than the microgroove control. However, loss-of-function transfections did not lead to significantly lower expressions than the microgroove control. These results indicate that, while pre-miR-27 and anti-miR-145 attenuate the effects of microgrooves, they do not negate all of these effects.

3.5 Chapter 3 discussion

Through TaqMAN RT-qPCR, miRNAs miR-27 and miR-145 were identified from a set of myomiRs and myogenesis-related miRNA as important regulators for microgroove induction of VSMC differentiation. miR-27 was significantly downregulated by microgroove shape modulation while miR-145 was significantly upregulated, marking both for further investigations. Gain-of-function and loss-of-function experiments proved that the two miRNAs indeed affect VSMC phenotype, producing opposing effects with miR-27 inhibiting SM marker genes and miR-145 promoting them. It is important to note that these miRNA do not account for the full effect of the microgrooves, despite their significant regulatory effect on VSMC differentiation. In Figs. 12 and 13 from Chapter 2 and Figs. 17 and 18, the microgroove induction has no significant effect on the expression of MHY11. However, anti-miR-27 and pre-miR-145 significantly promoted expression of MHY11, implying the diversion of molecular and physical effects. Comparing microgroove control trials to loss-of-function transfection trials also reflects this concept, as pre-miR-27 and anti-miR-145 can attenuate, but cannot negate the effects of

microgroove induction altogether. To further illustrate this point, microgroove/anti-miR-145 treatment still exhibits significantly higher expression of SM22 than flat control, but showed a lower SM22 level than the microgroove control. Also, anti-miR-145 significantly downregulated MYH11, while microgroove control had no significant effect on MYH11. In conclusion, microgrooves and miRNAs regulate the cellular processes in complex manners, but the understanding the roles of miR-27 and miR-145 does help delineate a part of the complex mechanisms.

The logical progression of inquiry would be to elucidate how miR-27 and miR-145 impact known pathways to promote VSMC phenotype in cells on microgroove. Literature provides possible explanations: Wang and Xu have found that miR-27 targets and inhibits adenomatous polyposis coli (APC) gene expression to promote osteoblast differentiation through canonical Wnt signaling.[47]. This suggests that in the early stages of SM differentiation, miR-27 may need to be downregulated in order to reprogram MSCs from the osteoblast lineage to the VSMC lineage. However, much more research is needed to test this possibility, and it is beyond the scope of this study. Considering that miRNAs often have multiple targets, computational prediction algorithms may provide another possible approach to identify targets of miR-27 most relevant to VSMC differentiation. Using miRDB developed by the Wang lab of Washington University, LIMK1 was identified as a potential target of miR-27. LIMK1 is notable for its role in phosphorylating and inactivating cofilin, which is an actin-binding protein that causes filament depolarization[54]. miR-27 may inhibit the formation of actin bundles through LIMK1, and downregulating miR-27 could promote the reorganization of the actin cytoskeleton to allow VSMC contractile function. Such targets could be validated by RT-qPCR and will be considered for future work.

In comparison to miR-27, miR-145's function is relatively well documented. miR-145 and miR-143 have been shown to cooperatively target Kruppel-like factor 4 (KLF4), myocardin (MYOCD) and ELK1, which is a member of the ETS oncogene family[35]. SRF and MYOCD promote the transcription of miR-145, which in turn directly targets and downregulates KLF4. KLF4 is a repressor of MYOCD, so miR-145 activity upregulates MYOCD, forming a positive feedback loop (Fig. 19). Future studies to validate the miR-145 promotion of VSMC differentiation shown in this study will focus on quantifying the expressions of KLF4 and MYOCD as a result of the microgroove induction.

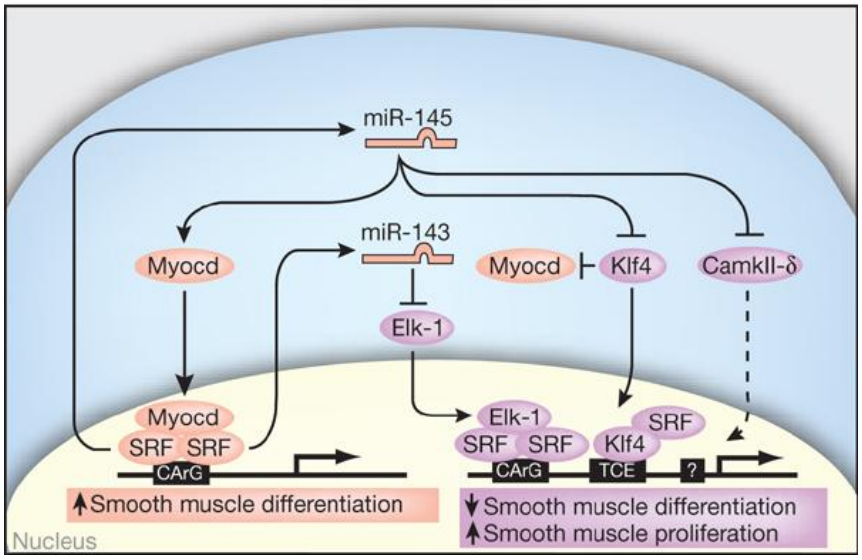

Fig. 19 - Role of miR-143 and miR-145 in VSMC differentiation
miR-143 and miR-15 cooperatively target ELK1, KLF4 and CaMKIIδ to induce smooth muscle differentiation towards the contractile phase and away from the synthetic phase. miR-145 targets KLF4 directly to promote MYOCD activity. (Adapted from Cordes et al.[35])

It is also important to note that miR-145 has been linked to biomechanical induction in previous studies. Chang et al. seeded microgrooves with VSMCs and reported significant increases of smooth muscle differentiation markers and miR-145[25]. Considering that microgrooves promoted contractile VSMC phenotype in dedifferentiated VSMCs, it is expected that similar regulatory factors such as miR-145 are also related to the microgroove-induction of MSC to VSMC differentiation. To advance the investigation further, regulators such as miR-27

and miR-145 were used to regulate the functional phenotype of flat and microgroove cultured MSCs in the following Chapter 4. The notion of using miRNA as therapeutic targets opens novel approaches to treat pathological forms of VSMC.

CHAPTER 4. MECHANICAL PHENOTYPE OF MSCs CULTURED ON MICROGROOVES AND miRNA TRANSFECTION

4.1 Abstract

Having identified the potential post-transcriptional regulators that mediate the induction of VSMC differentiation by shape anisotropy, this chapter evaluates the functional properties of MSC-SMC differentiation. Using microgroove-cultured MSCs with and without miRNA perturbations, the contractile abilities of the cells were compared to undifferentiated MSCs and VSMCs by measuring the cell traction force (CTF) with cell traction force microscopy (CTFM). The results showed that the repression of miR-27 and the promotion of miR-145 indeed led to the induction of VSMC-like contractile function, similar to the effects of microgroove culture. The inversed manipulations attenuated, though did not negate, the microgroove-induced differentiation. These findings further demonstrate the roles of miR-27 and miR-145 in the induction of VSMCs by shape anisotropy and suggest that these miRNAs provide viable options for therapeutic targeting to regulate VSMC phenotype.

4.2 Introduction

In response to the material properties of the environment and during migration, cells generate a traction force onto the adhered substrate. Measurement and quantification of these forces can provide insights into these mechanical processes. CTFM measures the displacement of the fluorescent beads embedded in a polyacrylamide hydrogel underlying the protein substrate (Fig. 20). At the end of the experiment, the cells are removed with trypsin and the gel returns to a null-force state. The displacements of the beads between the null-force and force-loaded states can be imaged by fluorescence microscopy and analyzed to calculate the CTFs.

While the traction forces can be interpreted as a 3D force, my study will focus on the traction forces as 2D as the main goal for comparison among experimental groups.

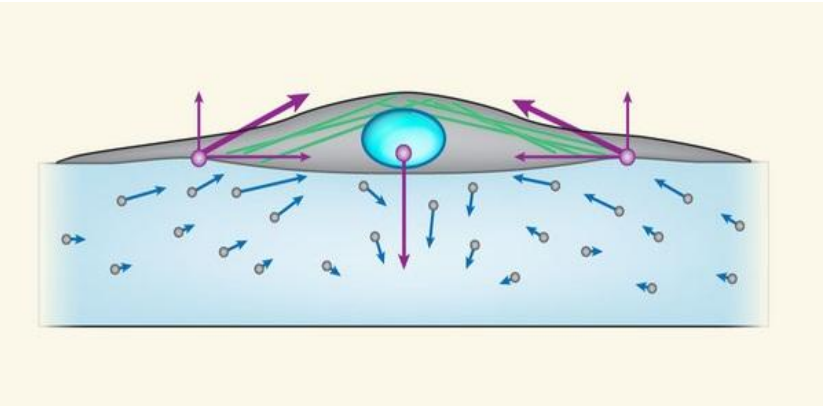

Fig. 20 - 3D forces of a cell on soft substrate
The 3D forces (purple) cause the displacements of the embedded beads (blue) through deformation of the gel. Traditionally the tangential forces along the surface are considered as the traction forces, though methods have been adapted for a 3D interpretation of the forces. (Adapted from Hersen et al.[55])

The CTFs originate from the contractile forces generated by the cytoskeleton structure and transmitted to the substrate through focal adhesion sites that are associated to the ends of cytoskeleton filaments. The focal adhesions are also attached to the substrate through integrin association with ECM proteins to generate the CTF at the substrate surface. The contractile forces are based on the interaction between motor protein myosin-II and the actin filaments of the cytoskeleton[56]. The head domain of myosin binds to the actin filament and uses the energy from ATP hydrolysis to move along the actin, pulling it in an anti-parallel direction. This process is the highly conserved basis for muscle contraction, as well as other forms of actin-based motility.

Since CTFs reflect the contractile tension of the cell, the functional VSMC contractile phenotype of the transfected MSCs can be assessed using CTFM. Chen et al. found that TGF-β stimulation of SMA in fibroblasts caused an increase of the CTF generated by the cells[57]. Furthermore, while SMA was not required for cells to generate CTFs, it has been shown that SMA expression enhanced CTF in a linear fashion[57]. Also, contractile force is an indicator of

increased activation of the RhoA/Rho-kinase (ROCK) pathway[58, 59]. ROCK phosphorylates MLC to induce myosin-actin interaction, which in turn activates myosin ATPase to provide the energy required for myosin contraction[58]. ROCK also promotes contraction by inhibiting MLC phosphatase, whose function is to deactivate MLC by dephosphorylation[60]. RhoA is a small GTPase which binds to ROCK activate its function [61, 62]. Rho not only is important to SM contraction, but also plays a role in the regulation of SMC differentiation, as demonstrated by the transcriptional activation of SRF [63]. Thus, further differentiation along the VSMC line to promote expressions of RhoA and SMA should translate into measureable development of contractility through CTFs.

4.3 Materials and methods

4.3.1 Cell culture

See sections 2.3.1-2.3.3 and 3.3.1.

4.3.2 PAG preparation

CTFM was used to compare the traction forces between MSCs, microgroove-seeded MSCs, and SMCs. To perform CTFM, I first fabricated an elastic polyacrymalide gel (PAG) substrate with embedded fluorescent beads[64]. A glass-bottomed Petri dish was treated with 0.1 M NaOH solution for 5 minutes, rinsed with ddH_20 and air-dried. 3-aminopropyltrimethoxysilane was added drop-wise onto the Petri dish and allowed to rest for 5 minutes before washing with ddH_20. The dish was then baked for 10 minutes at 37°C. The PAG solution was prepared starting with a mixture of 10% acrylamide/0.2% bis-acrylamide in a 4:1 ratio. The solution was mixed with 0.2 μm fluorescent beads that had been previously sonicated for 5 minutes to prevent bead aggregation. APS and TEMED were added and the mixture was poured into the pretreated Petri dish. A circular cover glass was placed over the solution and the gel was cured at room

temperature for 40 minutes before removing the cover glass. The PAG surface was covered by sulfo-SANPAH and the dish was exposed to UV light for 7 minutes to activate the sulfo-SANPAH crosslinker and to sanitize the gel. The PAG surface was then treated with 50 ng/µl of fibronectin overnight at 4°C. I determined the PAG thickness by calculating gel volume/gel area. The Young's modulus of 10% acrylamide and 0.2% bis-acrylamide PAG is typically ~6 kPa. The fibronectin was removed from the PAG, which is then rinsed with DPBS. The transfected MSCs were trypsinized from the flat and microgroove PDMS gels. Around 500-1,000 cells were then seeded on the PAG and allowed to set for 24 hours before imaging.

4.3.3 Image acquisition

I first found a field with only a single cell and took phase contrast images through a CCD camera attached onto a fluorescence microscope with 40x objective lens. Then, a z-stack of fluorescence images of the microbeads in the PAG was acquired as the force-loaded image set. The slide was then washed with DPBS and trypsinized to remove all cells from the PAG substrate. The PAG was imaged again for the reference z-stack at null-force state. The results were analyzed using a bead displacement mapping code that was developed by the del Álamo's Research Group in the Department of Mechanical and Aerospace Engineering of UC San Diego.

4.4 Results

4.4.1 SMCs show significantly larger CTFs than MSCs

CTFM was first used to compare the CTFs between SMCs and MSCs. The mean CTF for SMC was approximately twice as large as that of MSC (Fig. 21), indicating a clear difference in the contractile state of these cell types.

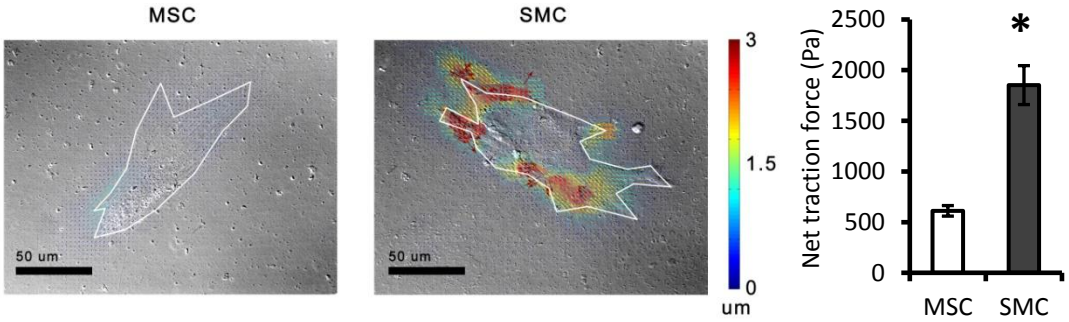

Fig. 21 - Net traction force of MSCs and SMCs
Phase contrast imaging on the left shows an individual MSC and SMC overlaid with the bead displacements measured by CTFM. The displacement magnitude is already clear in the SMC. Analysis of bead displacements reveal significant increase of net traction force in SMCs compared to MSCs ($p<0.05$).

4.4.2 Microgroove culture and transfection of pre-miR-145 and anti-miR-27 upregulate CTFs

CTFM was performed on six sample groups: (1) Microgroove and (2) flat cultured MSCs transfected with control molecules; Flat cultured MSCs transfected with either (3) pre-miR-145 or (4) anti-miR-27, and Microgroove-cultured MSCs transfected with either (5) anti-miR-145 or (6) pre-miR-27. Cells were randomly selected for CTFM, with the only requirement being that they were the only cell in the field of view. The cell-induced substrate deformation visualized by bead displacement showed the largest magnitudes in the microgroove control (1), flat pre-145 (3) and flat anti-27 (4), as denoted by the higher concentration of red arrows in Fig. 22 and the net traction forces quantified in Fig. 23.

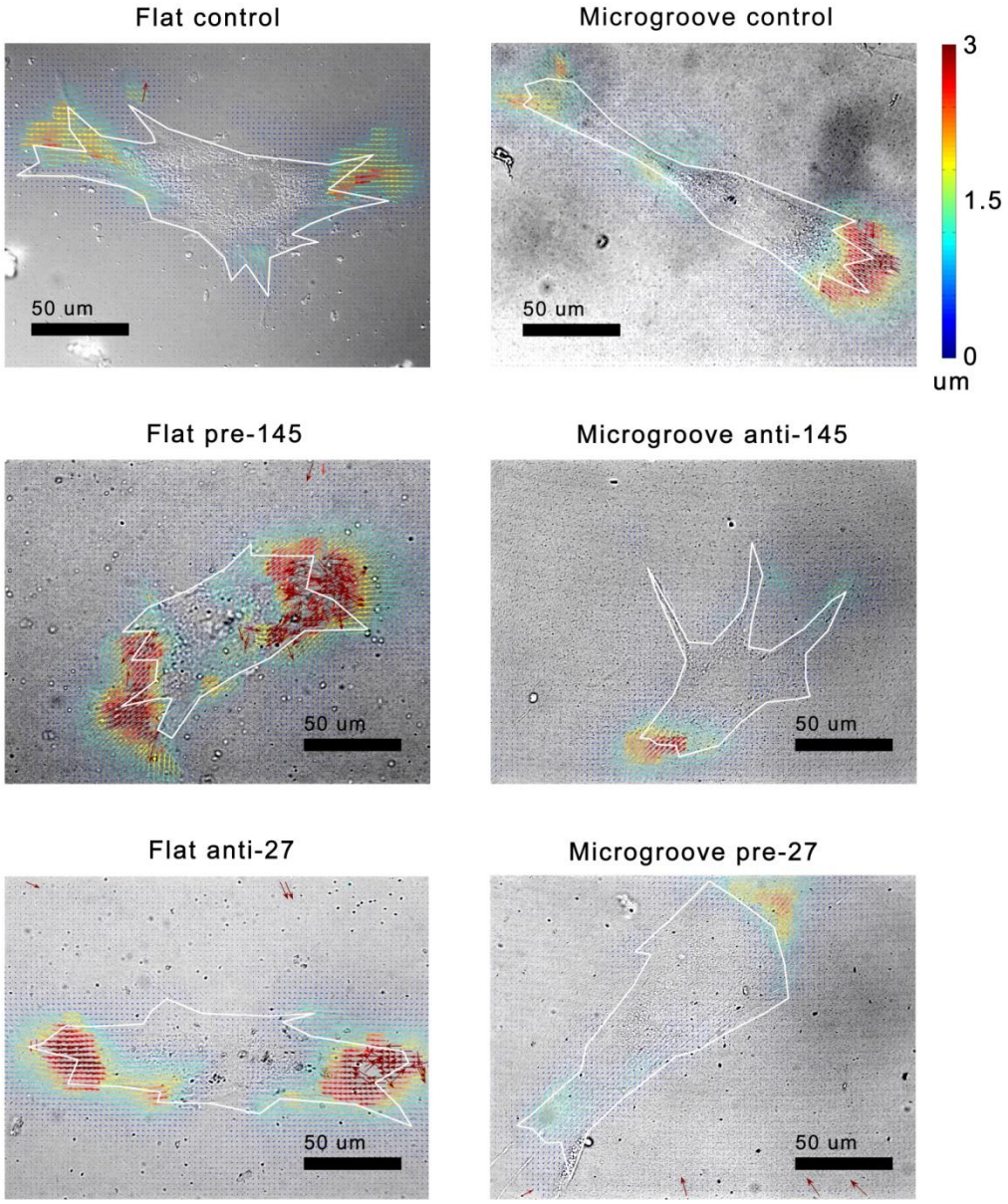

Fig. 22 - Displacement magnitudes for transfected flat and microgroove cultured MSCs
Phase images of the cells are overlapped with the calculated bead displacement magnitudes measured by CTFM. Red arrows representing larger magnitudes of displacement are more seen on the trials for MSCs cultured on microgroove with control transfection, flat with pre-145 transfection, and flat with anti-27 transfection.

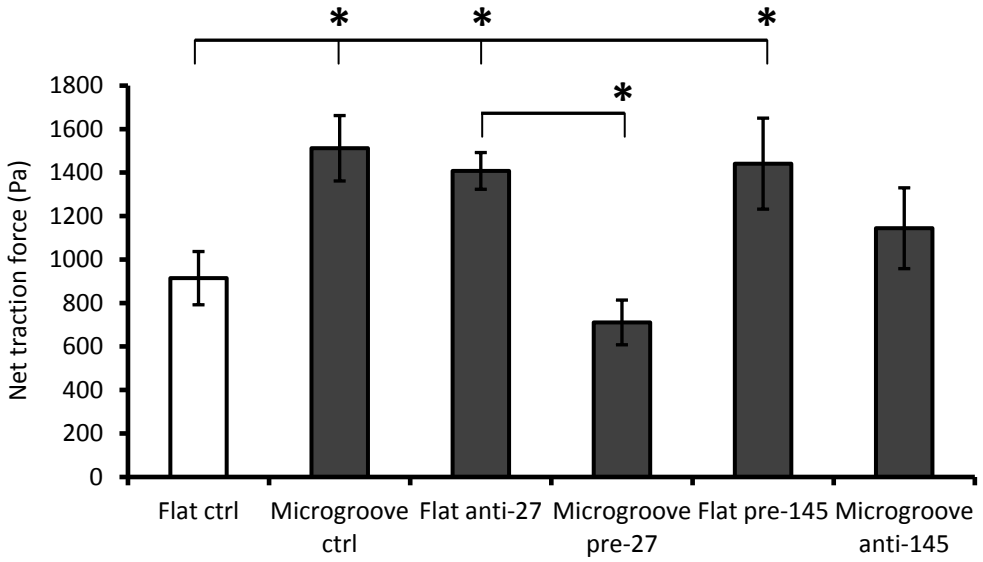

Fig. 23 - Net traction force of transfected MSCs cultured on flat and microgroove substrates
Analysis of bead displacements resulted in net traction forces of the various MSC culture conditions. Asterisks represent significant difference compared to flat cultured control sample ($p<0.05$).

The increase of net traction forces in the microgroove control over the flat control (Fig. 23, $p<0.05$) indicates a greater contractility and validates the results in Chapter 2. The significant increases of CTFs in flat culture following the transfections of anti-miR-27 and pre-miR-145 compared to flat control ($p<0.05$) are in agreement with the results seen in Chapter 3. The CTF for the microgroove-culture with pre-27 was significantly lower than that of the microgroove-culture control ($p<0.05$). The blockade of the effects of microgroove culture on CTF by pre-miR-27 is in agreement with the results of the loss-of-function experiments in Chapter 3, as pre-miR-27 can block the effects of microgroove culture to stimulate the CTF generated by the cell. However, the CTF of microgroove culture with anti-miR-145 is not significantly lower than that of microgroove control, nor is it significantly different from the flat control. These results suggest that the blockade of miR-145 does not completely abolish the effects of microgroove culture.

4.5 Chapter 4 Discussion

The utility of CTFM has broad applications in the study of cell motility, adhesion, growth, and differentiation. This research uses CTFM as a method to compare the state of contraction of the cell and, by extension, the VSMC functional phenotype. MSCs averaged 612 Pa in net traction force while SMCs averaged 1852 Pa. The results of the transfected and shape-modulated MSCs all fell within this range of force. Since they had all been cultured in media supplemented with TGF-β, some differentiation and contractile function was expected. Flat control averaged 914 Pa, closer to the MSC side of the differentiation spectrum while flat anti-miR-27 and flat pre-miR-145 groups were the closest to SMC CTF values at 1408 and 1441 Pa, respectively. Considering the range between MSCs and SMCs, even the most effective of the trials in this study only achieved about 60% of the SMC functional ability. This indicates that the culture conditions used on the MSCs only produced SMC-like cells that do not attain the full functional ability of SMCs. However, the results are successful in proving the relevance of cell shape in SMC differentiation, as well as the effects of miR-27 and miR-145.

The differences in CTF results among the MSC culture conditions can be related to the differences in SM gene expression. Given the linear relationship of SMA with CTF[57], the results of CTFM analysis suggest that the microgroove and transfection cultures have significant effects on the expression of SMA. This is also in agreement with the results reported in Chapter 2, where the channel width had the most significant effect on SMA expression (Fig. 6). Also, increased contractile ability suggests the activation of the RhoA/ROCK pathway, which not only activates myosin contraction, but also plays a role in SMC differentiation and actin reorganization[54, 65]. ROCK increases actin stabilization through indirect deactivation of cofilin, an actin-depolymerizing protein[54]. Higher levels of RhoA would help stabilize the alignment of actin filaments aligned by microgrooves, increasing the cell CTF and maintaining its elongated

shape. Future work is needed to elucidate the role of RhoA/ROCK in microgroove mediated VSMC differentiation.

An important consideration for the CTFM protocol was the cell shape on PAG gels. Current CTFM methods can include the micropatterning of the ECM surface coating, allowing for manipulation of the cell shape during CTFM imaging[66]. The advantage of this technique is that sample groups that were cultured on the microgrooves could retain their anisotropic shape during imaging while the groups cultured on flat substrate could be seeded normally. However, Oakes et al. showed that the magnitude of CTFs using a single type of fibroblast could be regulated by cell shape alone[67]. The local curvature of the cell is sufficient to regulate the magnitude of CTFs while factors such as substrate stiffness and the number of focal adhesions have relatively little effect due to the inherent mechanical nature of adherent cells[67]. Thus, micropatterning CTFM gels for the microgroove trials would inherently increase the magnitude of CTFs due to the cellular mechanics. Hence, it is better to simply compare both microgroove- and flat-cultured MSCs on non-patterned PAGs as the difference in CTFs between trials would better reflect differences in VSMC phenotype such as contractile protein expression and actin organization by not factoring the mechanical effects of cell shape into account. However, this also means that the contractile ability of the microgroove-cultured MSCs is higher in the microgrooves than what was detected through CTFM.

CHAPTER 5. CONCLUSIONS AND FUTURE WORK

5.1 Conclusion

Pathological dedifferentiation of VSMCs plays an important role in the development of atherosclerotic lesions and restenosis post-angioplasty. It has been observed that VSMCs in these conditions lose their contractile form and promote proliferation and migration at the lesion site. These changes lead to the threat of arterial thrombosis, which can jeopardize the patient's life. There is a current need to better understand the mechanisms that regulate the phenotype of VSMCs. There are needs for careful considerations of both biochemical and biomechanical factors that can modulate VSMC differentiation. While there have been many studies on biochemical differentiation, these *in vitro* studies generally do not incorporate the biomechanical factors existing *in vivo*. Recent studies on the effects of shape modulation on VSMCs, as well as the native shape of contractile VSMC, suggest that cell shape is also important for MSC-to-VSMC differentiation. There is a need to elucidate the underlying mechanisms on how biomechanical effects result in changes of cellular gene expression. miRNAs are novel post-transcriptional regulators that may be the missing link to understand VSMC gene expression pathways. This study was undertaken to delineate the effects of the shape anisotropy induced by PDMS microgrooves on the regulation of VSMC gene expression and provide deeper insight to the mechanisms involved.

The aims of this thesis are (1) to validate the capability of microgroove culture to stimulate VSMC gene expression, (2) to identify and validate mechano-sensitive miRNAs that regulate MSC phenotype as a result of shape modulation, and (3) to assess the functional phenotype of MSCs in response to modulations of shape and miRNA expression. In Chapter 2, shape anisotropy was systematically induced on MSC cultures by microgrooves with different widths manufactured through soft-lithography. The microgrooves were proven to successfully

modulate cell shape by restricting cell spreading in the direction perpendicular to the channels. This biomechanical stimulus combined with the biochemical effect of TGF-β resulted in significant upregulation of certain VSMC marker genes, particularly SMA, as reflected by RT-qPCR and Western blot. My results also indicate that SMA expression increased as the microgroove channel width decreased.

The focus of Chapter 3 was to identify the miRNAs that regulate the microgroove-mediated differentiation. By profiling a whole set of myogenesis-related miRNA, miR-27 and miR-145 were selected as potential regulators with opposite effects: miR-27 was downregulated by microgroove culture, while miR-145 was upregulated. The abilities of miR-27 and miR-145 to inhibit and promote VSMC function, respectively, was validated by performing gain-of-function and loss-of-function experiments. The results showed that gain-of-function transfection of anti-miR-27 and pre-miR-145 upregulated VSMC marker genes, making the expression pattern on flat cultures resemble those cultured on microgroove gels. The loss-of-function experiments showed the other side of the coin as pre-miR-27 and anti-miR-145 partially negated the effects of microgroove culture. These results confirmed the roles of miR-27 and miR-145 as key regulators of the microgroove-induction of the VSMC phenotype.

In Chapter 4, the results of Chapters 2 and 3 were further validated by CTFM, which provides the biomechanical information on VSMC phenotype. Comparison of the CTF results showed that the VSMCs had higher contractility than MSCs. I also found that both microgrooves and gain-of-function transfections significantly increased CTFs, while loss-of-function transfections generally attenuated them. Since CTFs have been linked to contractile function, the results suggest greater expression of SMA and activation of the RhoA/ROCK pathway. Thus, miR-27 and miR-145 could be therapeutic targets of interest to regulate VSMC phenotype *in vivo* where regulation by biomechanical stimuli would be difficult to achieve.

Overall, my studies demonstrate the importance of biomechanical forces on VSMC differentiation. The novel findings of this work include 1) microgroove induction of MSC to VSMC gene expression, 2) identification of miR-27 and miR-145 as regulators of microgroove induction, and 3) validation of the abilities of shape modulation and microRNAs (miR-27 and miR-145) to influence the contractile phenotype of MSCs. The findings of this study have implications on a broad range of bioengineering applications, including novel treatments of atherosclerotic lesions, construction of tissue engineering grafts, and differentiation of stem cells to VSMCs.

5.2 Future work

While I showed that microgrooves have significant morphological effects on MSCs, another important parameter that was not addressed was cell orientation. To round out the data, future studies will include quantification of cell orientation by using the directionality of the f-actin fibers and analysis by ImageJ. As shown in Chapters 2 and 4, microgrooves upregulate certain SM markers and promote contractile function. The validation of RhoA/ROCK pathway activation would round out the findings of both Chapters, given its regulatory role in myosin contraction, actin organization and VSMC differentiation. Western blot of MLCK would provide valuable insight on how RhoA responds to biomechanical induction. Gain-of-function and loss-of-function experiments can be repeated for MLCK to indentify whether miR-27 and miR-145 regulate microgroove induction through the RhoA/ROCK pathway. Repetition of certain Western blots throughout Chapter 2 and 3 would also help reduce some of the uncertainties in my results.

To expand on the results of Chapter 3, the effect of miRNA modulation could be further examined by combining miR-27 and miR-145 in MSC transfection. Using both miRNA may

produce stronger gain-of-function or loss-of-function results to better induce SM markers or inhibit microgroove-induced changes. Given the importance of miR-27 and mir-145, it is also valuable to validate the key targets that result in VSMC phenotype. KLF4, MYOCD, and ELK1 have previously been connected to miR-143 and 145 in directing SMC plasticity and should be validated by western blot. miR-27 is more difficult to study, since potential targets have not yet been verified, but computational prediction may lead to important targets such as LIMK1.

Finally, future studies could assess the abilities of miR-27 and miR-145 to affect VSMC phenotype *in vivo*. By using the perturbed rat carotid artery model, anti-miR-27 or pre-miR-145 can be delivered to atherosclerotic regions with aid of nanoparticles. The results of these studies may provide novel therapeutic treatment methods for atherosclerotic lesions.

5.3 Closing Remarks

This work is original. The primary investigator and author of this thesis was Joshua Wei.

REFERENCES

1. Tahergorabi, Z. and M. Khazaei, *A Review on Angiogenesis and Its Assays.* Iran J Basic Med Sci, 2012. **15**(6): p. 1110-26.

2. Dominici, M., K. Le Blanc, I. Mueller, I. Slaper-Cortenbach, F.C. Marini, D.S. Krause, R.J. Deans, A. Keating, D.J. Prockop, and E.M. Horwitz, *Minimal criteria for defining multipotent mesenchymal stromal cells. The International Society for Cellular Therapy position statement.* Cytotherapy. **8**(4): p. 315-317.

3. Majesky, M.W., X.R. Dong, J.N. Regan, and V.J. Hoglund, *Vascular Smooth Muscle Progenitor Cells: Building and Repairing Blood Vessels.* Circulation Research, 2011. **108**(3): p. 365-377.

4. Owens, G.K., *Regulation of differentiation of vascular smooth muscle cells.* Physiological Reviews, 1995. **75**(3): p. 487-517.

5. Owens, G.K., M.S. Kumar, and B.R. Wamhoff, *Molecular Regulation of Vascular Smooth Muscle Cell Differentiation in Development and Disease.* Physiological Reviews, 2004. **84**(3): p. 767-801.

6. Milewicz, D.M., C.S. Kwartler, C.L. Papke, E.S. Regalado, J. Cao, and A.J. Reid, *Genetic variants promoting smooth muscle cell proliferation can result in diffuse and diverse vascular diseases: Evidence for a hyperplastic vasculomyopathy.* Genet Med, 2010. **12**(4): p. 196-203.

7. Wang, Z., D.-Z. Wang, G.C.T. Pipes, and E.N. Olson, *Myocardin is a master regulator of smooth muscle gene expression.* Proceedings of the National Academy of Sciences, 2003. **100**(12): p. 7129-7134.

8. Miano, J.M., *Serum response factor: toggling between disparate programs of gene expression.* Journal of Molecular and Cellular Cardiology, 2003. **35**(6): p. 577-593.

9. Pipes, G.C.T., E.E. Creemers, and E.N. Olson, *The myocardin family of transcriptional coactivators: versatile regulators of cell growth, migration, and myogenesis.* Genes & Development, 2006. **20**(12): p. 1545-1556.

10. Scharenberg, M.A., B.E. Pippenger, R. Sack, D. Zingg, J. Ferralli, S. Schenk, I. Martin, and R. Chiquet-Ehrismann, *TGF-β-induced differentiation into myofibroblasts involves specific regulation of two MKL1 isoforms.* Journal of Cell Science, 2014.

11. Gong, Z. and L.E. Niklason, *Small-diameter human vessel wall engineered from bone marrow-derived mesenchymal stem cells (hMSCs).* The FASEB Journal, 2008. **22**(6): p. 1635-1648.

12. Wang, D., J.S. Park, J.S.F. Chu, A. Krakowski, K. Luo, D.J. Chen, and S. Li, *Proteomic Profiling of Bone Marrow Mesenchymal Stem Cells upon Transforming Growth Factor β1 Stimulation.* Journal of Biological Chemistry, 2004. **279**(42): p. 43725-43734.

13. Yamashita, J., H. Itoh, M. Hirashima, M. Ogawa, S. Nishikawa, T. Yurugi, M. Naito, K. Nakao, and S.-I. Nishikawa, *Flk1-positive cells derived from embryonic stem cells serve as vascular progenitors.* Nature, 2000. **408**(6808): p. 92-96.

14. Merfeld-Clauss, S., I.P. Lupov, H. Lu, D. Feng, P. Compton-Craig, K.L. March, and D.O. Traktuev, *Adipose Stromal Cells Differentiate Along a Smooth Muscle Lineage Pathway Upon Endothelial Cell Contact via Induction of Activin A.* Circulation Research, 2014. **115**(9): p. 800-809.

15. Cheung, C., A.S. Bernardo, R.A. Pedersen, and S. Sinha, *Directed differentiation of embryonic origin–specific vascular smooth muscle subtypes from human pluripotent stem cells.* Nat. Protocols, 2014. **9**(4): p. 929-938.

16. Augello, A. and C. De Bari, *The Regulation of Differentiation in Mesenchymal Stem Cells.* Human Gene Therapy, 2010. **21**(10): p. 1226-1238.

17. Mammoto, A., T. Mammoto, and D.E. Ingber, *Mechanosensitive mechanisms in transcriptional regulation.* Journal of Cell Science, 2012. **125**(13): p. 3061-3073.

18. Kurpinski, K., J. Chu, C. Hashi, and S. Li, *Anisotropic mechanosensing by mesenchymal stem cells.* Proceedings of the National Academy of Sciences, 2006. **103**(44): p. 16095-16100.

19. Heo, S.-J., S.D. Thorpe, T.P. Driscoll, R.L. Duncan, D.A. Lee, and R.L. Mauck, *Biophysical Regulation of Chromatin Architecture Instills a Mechanical Memory in Mesenchymal Stem Cells.* Scientific Reports, 2015. **5**: p. 16895.

20. Lee, J., A.A. Abdeen, and K.A. Kilian, *Rewiring mesenchymal stem cell lineage specification by switching the biophysical microenvironment.* Scientific Reports, 2014. **4**: p. 5188.

21. Stary, H.C., A.B. Chandler, R.E. Dinsmore, V. Fuster, S. Glagov, W. Insull, M.E. Rosenfeld, C.J. Schwartz, W.D. Wagner, and R.W. Wissler, *A Definition of Advanced Types of Atherosclerotic Lesions and a Histological Classification of Atherosclerosis: A Report From the Committee on Vascular Lesions of the Council on Arteriosclerosis, American Heart Association.* Circulation, 1995. **92**(5): p. 1355-1374.

22. Groot, A.C.G.-d., M.C. DeRuiter, M. Bergwerff, and R.E. Poelmann, *Smooth Muscle Cell Origin and Its Relation to Heterogeneity in Development and Disease.* Arteriosclerosis, Thrombosis, and Vascular Biology, 1999. **19**(7): p. 1589-1594.

23. Schwartz, S.M., *Perspectives series: cell adhesion in vascular biology. Smooth muscle migration in atherosclerosis and restenosis.* J Clin Invest, 1997. **99**(12): p. 2814-6.

24. Fuster, V., P.R. Moreno, Z.A. Fayad, R. Corti, and J.J. Badimon, *Atherothrombosis and High-Risk Plaque: Part I: Evolving Concepts.* Journal of the American College of Cardiology, 2005. **46**(6): p. 937-954.

25. Chang, S., S. Song, J. Lee, J. Yoon, J. Park, S. Choi, J.-K. Park, K. Choi, and C. Choi, *Phenotypic Modulation of Primary Vascular Smooth Muscle Cells by Short-Term Culture on Micropatterned Substrate.* PLoS ONE, 2014. **9**(2): p. e88089.

26. Sayed, D. and M. Abdellatif, *MicroRNAs in Development and Disease.* Physiological Reviews, 2011. **91**(3): p. 827-887.

27. Carthew, R.W. and E.J. Sontheimer, *Origins and Mechanisms of miRNAs and siRNAs.* Cell, 2009. **136**(4): p. 642-655.

28. Kim, V.N., *MicroRNA biogenesis: coordinated cropping and dicing.* Nat Rev Mol Cell Biol, 2005. **6**(5): p. 376-385.

29. Chendrimada, T.P., R.I. Gregory, E. Kumaraswamy, J. Norman, N. Cooch, K. Nishikura, and R. Shiekhattar, *TRBP recruits the Dicer complex to Ago2 for microRNA processing and gene silencing.* Nature, 2005. **436**(7051): p. 740-744.

30. McCarthy, J.J., *The MyomiR Network in Skeletal Muscle Plasticity.* Exercise and Sport Sciences Reviews, 2011. **39**(3): p. 150-154.

31. Sempere, L.F., S. Freemantle, I. Pitha-Rowe, E. Moss, E. Dmitrovsky, and V. Ambros, *Expression profiling of mammalian microRNAs uncovers a subset of brain-expressed microRNAs with possible roles in murine and human neuronal differentiation.* Genome Biol, 2004. **5**(3): p. R13.

32. Bang, C., J.A.N. Fiedler, and T. Thum, *Cardiovascular Importance of the MicroRNA-23/27/24 Family.* Microcirculation, 2012. **19**(3): p. 208-214.

33. Crist, C.G., D. Montarras, G. Pallafacchina, D. Rocancourt, A. Cumano, S.J. Conway, and M. Buckingham, *Muscle stem cell behavior is modified by microRNA-27 regulation of Pax3 expression.* Proc Natl Acad Sci U S A, 2009. **106**(32): p. 13383-7.

34. Goupille, O., G. Pallafacchina, F. Relaix, S.J. Conway, A. Cumano, B. Robert, D. Montarras, and M. Buckingham, *Characterization of Pax3-expressing cells from adult blood vessels.* J Cell Sci, 2011. **124**(23): p. 3980-8.

35. Cordes, K.R., N.T. Sheehy, M.P. White, E.C. Berry, S.U. Morton, A.N. Muth, T.-H. Lee, J.M. Miano, K.N. Ivey, and D. Srivastava, *miR-145 and miR-143 regulate smooth muscle cell fate and plasticity.* Nature, 2009. **460**(7256): p. 705-710.

36. Cheng, Y., X. Liu, J. Yang, Y. Lin, D.-Z. Xu, Q. Lu, E.A. Deitch, Y. Huo, E.S. Delphin, and C. Zhang, *MicroRNA-145, a Novel Smooth Muscle Cell Phenotypic Marker and Modulator, Controls Vascular Neointimal Lesion Formation.* Circulation Research, 2009. **105**(2): p. 158-166.

37. Rensen, S., P. Doevendans, and G. van Eys, *Regulation and characteristics of vascular smooth muscle cell phenotypic diversity.* Neth Heart J, 2007. **15**(3): p. 100-8.

38. Liu, N., S. Bezprozvannaya, A.H. Williams, X. Qi, J.A. Richardson, R. Bassel-Duby, and E.N. Olson, *microRNA-133a regulates cardiomyocyte proliferation and suppresses smooth muscle gene expression in the heart.* Genes Dev, 2008. **22**(23): p. 3242-54.

39. Yang, L.-x., G. Liu, G.-f. Zhu, H. Liu, R.-w. Guo, F. Qi, and J.-h. Zou, *MicroRNA-155 inhibits angiotensin II-induced vascular smooth muscle cell proliferation.* Journal of Renin-Angiotensin-Aldosterone System, 2014. **15**(2): p. 109-116.

40. Thakar, R.G., Q. Cheng, S. Patel, J. Chu, M. Nasir, D. Liepmann, K. Komvopoulos, and S. Li, *Cell-Shape Regulation of Smooth Muscle Cell Proliferation.* Biophys J, 2009. **96**(8): p. 3423-32.

41. Mata, A., A.J. Fleischman, and S. Roy, *Characterization of Polydimethylsiloxane (PDMS) Properties for Biomedical Micro/Nanosystems.* Biomedical Microdevices. **7**(4): p. 281-293.

42. Chase, L.G., S. Yang, V. Zachar, Z. Yang, U. Lakshmipathy, J. Bradford, S.E. Boucher, and M.C. Vemuri, *Development and Characterization of a Clinically Compliant Xeno-Free Culture Medium in Good Manufacturing Practice for Human Multipotent Mesenchymal Stem Cells.* Stem Cells Transl Med, 2012. **1**(10): p. 750-8.

43. Suárez, Y., C. Fernández-Hernando, J.S. Pober, and W.C. Sessa, *Dicer Dependent MicroRNAs Regulate Gene Expression and Functions in Human Endothelial Cells.* Circulation Research, 2007. **100**(8): p. 1164-1173.

44. Kuehbacher, A., C. Urbich, A.M. Zeiher, and S. Dimmeler, *Role of Dicer and Drosha for Endothelial MicroRNA Expression and Angiogenesis.* Circulation Research, 2007. **101**(1): p. 59-68.

45. Hua, Z., Q. Lv, W. Ye, C.K.A. Wong, G. Cai, D. Gu, Y. Ji, C. Zhao, J. Wang, B.B. Yang, and Y. Zhang, *MiRNA-Directed Regulation of VEGF and Other Angiogenic Factors under Hypoxia.* PLoS ONE, 2006. **1**(1).

46. McDaneld, T.G., T.P.L. Smith, M.E. Doumit, J.R. Miles, L.L. Coutinho, T.S. Sonstegard, L.K. Matukumalli, D.J. Nonneman, and R.T. Wiedmann, *MicroRNA transcriptome profiles during swine skeletal muscle development.* BMC Genomics, 2009. **10**: p. 77.

47. Wang, T. and Z. Xu, *miR-27 promotes osteoblast differentiation by modulating Wnt signaling.* Biochemical and Biophysical Research Communications, 2010. **402**(2): p. 186-189.

48. Nielsen, S., C. Scheele, C. Yfanti, T. Åkerström, A.R. Nielsen, B.K. Pedersen, and M. Laye, *Muscle specific microRNAs are regulated by endurance exercise in human skeletal muscle.* J Physiol, 2010. **588**(Pt 20): p. 4029-37.

49. Chen, J.F., E.M. Mandel, J.M. Thomson, Q. Wu, T.E. Callis, S.M. Hammond, F.L. Conlon, and D.Z. Wang, *The role of microRNA-1 and microRNA-133 in skeletal muscle proliferation and differentiation.* Nat Genet, 2006. **38**(2): p. 228-33.

50. McCarthy, J.J., K.A. Esser, C.A. Peterson, and E.E. Dupont-Versteegden, *Evidence of MyomiR network regulation of β-myosin heavy chain gene expression during skeletal muscle atrophy.* Physiological Genomics, 2009. **39**(3): p. 219-226.

51. Rangrez, A.Y., Z.A. Massy, V. Metzinger-Le Meuth, and L. Metzinger, *miR-143 and miR-145: Molecular Keys to Switch the Phenotype of Vascular Smooth Muscle Cells.* Circulation: Cardiovascular Genetics, 2011. **4**(2): p. 197-205.

52. Kim, S. and H. Iwao, *Molecular and Cellular Mechanisms of Angiotensin II-Mediated Cardiovascular and Renal Diseases.* Pharmacological Reviews, 2000. **52**(1): p. 11-34.

53. Liu, Y., J. Wen, L. Dong, B. Zheng, and M. Han, *Krüppel-like factor (KLF) 5 mediates cyclin D1 expression and cell proliferation via interaction with c-Jun in Ang II-induced VSMCs.* Acta Pharmacol Sin, 2010. **31**(1): p. 10-8.

54. Riento, K. and A.J. Ridley, *ROCKs: multifunctional kinases in cell behaviour.* Nat Rev Mol Cell Biol, 2003. **4**(6): p. 446-456.

55. Hersen, P. and B. Ladoux, *Biophysics: Push it, pull it.* Nature, 2011. **470**(7334): p. 340-341.

56. Harris, G., *Molecular biology of the cell by Bruce Alberts, Dennis Bray, Julian Lewis, Martin Raff , Keith Roberts and James D. Watson, Garland Publishing, 1983.* Immunol Today, 1983. **4**(12): p. 352.

57. Chen, J., H. Li, N. SundarRaj, and J.H.C. Wang, *Alpha-smooth muscle actin expression enhances cell traction force.* Cell Motility and the Cytoskeleton, 2007. **64**(4): p. 248-257.

58. Amano, M., M. Ito, K. Kimura, Y. Fukata, K. Chihara, T. Nakano, Y. Matsuura, and K. Kaibuchi, *Phosphorylation and Activation of Myosin by Rho-associated Kinase (Rho-kinase).* Journal of Biological Chemistry, 1996. **271**(34): p. 20246-20249.

59. Pirone, D.M., W.F. Liu, S.A. Ruiz, L. Gao, S. Raghavan, C.A. Lemmon, L.H. Romer, and C.S. Chen, *An inhibitory role for FAK in regulating proliferation: a link between limited adhesion and RhoA-ROCK signaling.* The Journal of Cell Biology, 2006. **174**(2): p. 277-288.

60. Wang, Y., X.R. Zheng, N. Riddick, M. Bryden, W. Baur, X. Zhang, and H.K. Surks, *ROCK Isoform Regulation of Myosin Phosphatase and Contractility in Vascular Smooth Muscle Cells.* Circ Res, 2009. **104**(4): p. 531-40.

61. Leung, T., E. Manser, L. Tan, and L. Lim, *A Novel Serine/Threonine Kinase Binding the Ras-related RhoA GTPase Which Translocates the Kinase to Peripheral Membranes.* Journal of Biological Chemistry, 1995. **270**(49): p. 29051-29054.

62. Amano, M., M. Nakayama, and K. Kaibuchi, *Rho-Kinase/ROCK: A Key Regulator of the Cytoskeleton and Cell Polarity.* Cytoskeleton (Hoboken), 2010. **67**(9): p. 545-54.

63. Hill, C.S., J. Wynne, and R. Treisman, *The Rho family GTPases RhoA, Racl , and CDC42Hsregulate transcriptional activation by SRF.* Cell, 1995. **81**(7): p. 1159-1170.

64. Wang, J.-C. and B. Li, *Application of Cell Traction Force Microscopy for Cell Biology Research*, in *Cytoskeleton Methods and Protocols*, R.H. Gavin, Editor. 2010, Humana Press. p. 301-313.

65. Mack, C.P., A.V. Somlyo, M. Hautmann, A.P. Somlyo, and G.K. Owens, *Smooth Muscle Differentiation Marker Gene Expression Is Regulated by RhoA-mediated Actin Polymerization.* Journal of Biological Chemistry, 2001. **276**(1): p. 341-347.

66. Burnham, M.R., J.N. Turner, D. Szarowski, and D.L. Martin, *Biological functionalization and surface micropatterning of polyacrylamide hydrogels.* Biomaterials, 2006. **27**(35): p. 5883-5891.

67. Oakes P , W., S. Banerjee, C. Marchetti M , and L. Gardel M *Geometry Regulates Traction Stresses in Adherent Cells.* Biophys J, 2014. **107**(4): p. 825-33.